Deep-water massive sands: Facies, processes and channel geometry in the Numidian Flysch, Sicily

Article *in* Sedimentary Geology · January 1998

DOI: 10.1016/S0037-0738(97)00095-X

ELSEVIER

Marine and Petroleum Geology 17 (2000) 145–174

Marine and Petroleum Geology

Deep-water massive sands: nature, origin and hydrocarbon implications

Dorrik A.V. Stow[a,*], Melissa Johansson[b]

[a]*School of Ocean and Earth Science, Southampton Oceanography Centre, The University, Waterfront Campus, Southampton SO14 3ZH, UK*
[b]*Schlumberger, Rohas Perkasa, No 8 Jala Perak, Kuala Lumpur, 50456, Malaysia*

Received 23 November 1998; received in revised form 13 August 1999; accepted 16 August 1999

Abstract

Deep-water massive sands (DWMS) are here defined as very thick (>1 m) sand beds or units that are devoid of primary sedimentary structures and that occur in association with other deep-water sediments — the massive sand facies association. Following careful examination of some 70 examples of massive sands drawn from deep-water successions of all ages and lithologies, we are confident that the shroud of mystery surrounding these deposits can be lifted, their origin and nature can be explained and their importance as hydrocarbon reservoirs can be brought sharply into focus.

Besides their very thick bedding and structureless aspect, key features of DWMSs are the common presence of water escape structures, subtle amalgamation surfaces and shale clasts. Typically they show poor to moderate sorting and compositional immaturity. The two key processes involved in their long-distance transport and emplacement are sandy debris flows (SDFs) and high-density turbidity currents (HDTs). Post-depositional liquefaction and sand injection can significantly affect either type. They generally occur as part of a thicker sand-dominated sequence or sand body (sand/shale ratios 7:1 to >9:1) fed from a clean sand and/or gravel-rich source. The variety of scales and geometries is dependent upon the depositional setting: chutes, scours, flow-slides and lobe sheets on smaller-scale fan-deltas; channel, ribbon and tongue-like bodies on open slopes and proximal fans; lobate and lensoid bodies more distally; and trough/basin sand bodies that are broadly lensoid to tabular. The process/facies type and depositional setting profoundly affect both the internal architecture and external geometry of DWMS bodies.

1. Introduction

1.1. The massive sands problem

Thick sequences of massive sands and sandstones (DWMS) are commonly found associated with turbidites, mainly in ancient sedimentary successions. In many cases, they form important subsurface reservoirs for hydrocarbons. However, their nature, variety and geometry have been poorly documented and, consequently, their origins have posed an important problem for students of deep-water sedimentation (Johansson, Braakenburg, Stow & Faugeres, 1998; Kneller, 1995; Kneller & Branney, 1995; Stow, Braakenburg & Johansson, 1995; Stow, Reading & Collinson 1996).

Recent discoveries of hydrocarbons in such sands include a number of Paleogene fields in the North Sea (e.g. Alba, Gryphon, Balder, Frigg, Heimdal, Forties, Montrose, Arbroath, Andrew), several Mesozoic North Sea fields (e.g. Agat, Kopervik, Galley, Claymore, Scapa, Songefjord and part of the Brae–Miller complex), and Cretaceous discoveries offshore central and northern Norway. Currently, active exploration programmes in deeper water continental margin areas have led to numerous discoveries of oil and gas in Tertiary DWMS and associated turbidite plays offshore Brazil (e.g. Marlim, Carapeba, Macae and others in

* Corresponding author. Tel.: +44-1703-595-000; fax: +44-1703-593-052.
E-mail address: dorrik.a.v.stow@soc.soton.ac.uk (D.A.V. Stow).

0264-8172/00/$ - see front matter
PII: S0264-8172(99)00051-3

the Campos Basin), offshore west Africa (e.g. Baudroie, Baliste, Zafiro, Opalo), west of Shetlands (Foinhaven, Schiehallion), and in the Gulf of Mexico ponded slope basins. For a summary review of the world's principal turbidite plays, many of which include DWMS reservoirs, see Pettingill (1998).

These discoveries have led to much interest and a multitude of partial and speculative theories for their origin, including giant sandy debris flows (Shanmugam, 1996; Shanmugam et al., 1994) and the bottom current shaping of sand mounds (Enjolras, Gouadain, Mutti & Pizon, 1986; Mutti, Barros, Possato & Rumenos, 1980). From previous work on ancient successions, there are at least three main interpretations of the depositional settings in which massive sands occur. These are: (1) the slope-apron gully-lobe system, exemplified by the Jurassic Hareelv Formation of eastern Greenland (Surlyk, 1987); (2) the delta-fed ramp system, proposed for the Cretaceous Tyee Formation of Oregon and the Paleogene Matilija Formation of California (Heller & Dickinson, 1985); and (3) the sand-rich submarine fan system, into which many previous workers have attempted to fit a variety of massive sand examples (e.g. Armstrong, Ten Have & Johnson, 1987; Busby-Spera, 1985; Carman & Young, 1981; Link & Nilsen, 1980).

In order to tackle this problem and arrive at a better understanding of deep-water massive sands, an industry-consortium study was formulated. Its specific remit was to: (1) survey the whole spectrum of massive sands of different ages and from different settings; and (2) document in detail the specific characteristics of a limited number of ancient case studies exposed on land. What we present here is a synthesis of the key features observed together with our interpretations in terms of processes of transport and deposition, facies geometry, vertical sequences and likely depositional setting. The observed features are illustrated from the range of examples studied, and more complete descriptions of individual case studies are and will be published separately (Johansson et al., 1998; Stow, Johansson, Braakenburg & Faugeres, 1999). We further consider the question of modern analogues and make preliminary comment on the relevance of the models developed to problems of exploration for and production from DWMS hydrocarbon reservoirs.

1.2. Definitions

Unfortunately, the term massive sand is used variously in the literature on deep-water deposits. Some authors emphasise the thickness, some the structureless aspect, and others consider both important. Thus, in some cases thin and medium-bedded Bouma AE turbidites have been referred to as massive sands and, in other cases, very thick borehole sequences that are uncored but display a 'uniform-sand' log response are so described. Clearly some uniformity of terminology is required. Wireline log character alone, we suggest is insufficient evidence for designation of a massive sand, although good quality FMS/FMI images may be allowable. In outcrops and cores, thin to thick-bedded structureless sands are not particularly unusual and can be readily interpreted in terms of Bouma or Lowe-type medium and coarse-grained turbidites (see Stow et al., 1996). It is the very thick structureless beds (>1 m and in some cases >10 m in thickness), that are rarer in occurrence and pose more of a problem in interpretation — it is these that we refer to as deep-water massive sands (DWMS). In fact, at the outset of this study we adopted the rather greater and somewhat arbitrary lower limit of bed thickness as 4 m, so that all our examples include at least some of these extra thick beds. However, we now propose a definition of a deep-water massive sand as a very thick (>1 m) sand bed that is essentially devoid of primary sedimentary structures and that occurs in association with other deep-water (deeper than storm-wave base) sediments, most commonly turbidites and hemipelagites. This definition does bring rather more deep-water sands into the DWMS family than was our original intention, but is more acceptable because >1 m is in line with the accepted terminology for a *very thick bed* and because many apparently thicker DWMS units are, in fact, made up of individual depositional beds 1 to 3 m thick.

With respect to massive sands, the term *bed* is used in its standard sense to mean a single identifiable stratum that is believed to have been deposited by one event. However, in many of the examples studied, a number of beds have clearly been amalgamated into a massive sandstone *unit* or *body*. Such units comprise, typically, from two to eight beds (rarely more). In some cases the surfaces of amalgamation are very poorly defined and can only be inferred from subtle changes in sandstone properties. In these cases, the distinction between a bed and a unit is less clear. Massive sandstone beds and units generally occur within a thicker succession of associated coarse and fine grained resedimented facies. This whole succession is referred to as the massive sandstone *complex*. In some cases, the complex is equivalent to a named geological Member or even Formation.

1.3. Database summary

This study has brought together data on 70 examples of deep-water massive sands from around the world. These range in age from Precambrian to Recent, and include siliciclastic, carbonate and volcani-

Table 1
Examples and key characteristics of deep-water massive sands and associated deposits used in this study[a]

Appendix reference	Example	Thickness (m)			Geometry (km)				Massive sand facies association (dominant)	Associated facies (encasing) (dominant)	Depositional setting (inferred)	Category
		Body	Unit	Bed	Length	Width	Volume (km^3)	Shape				
1.	Alba Fm*	0–120			11	1		Channel	MS	H, Ij	Base of slope (terrace/ ?channel	A–HC
2.	Bergamo Flysch			< 30	25	10	4–20	Sheet/lenticular	MB	T, H	Small, active basin	A–M
3.	Black Flysch	30–50						Lensoid sheet/elongate mound	MS, Tcg, D	Tfg, H	Channel	A
4.	Bray Sst*	< 100		1–7	60			Channel	MS, Tcg+fg	Tfg, H	Basin, narrow elongate	A
5.	Cabrillo Fm*			5–15				Channel	MS, Tcg+fg	Tfg	Mid fan, channel-fill	A
6.	Cantua Sst*	1000	< 25	2–15	40	15		Tabular	MS, T	T, H	Fault-bounded borderland basin	A–CS9
7.	Capistrano Fm*	100		< 10	1	< 1		Channel	MS, Tcg	Tfg	Fan channel	A
8.	Carapebus Fm*	av. 100						Mound	MS	Tcg Tfg	Slope	A–HC
9.	Chatsworth Fm*	< 1800		1–7	40	20		Broad lens, tabular	MS, T	T, H	Fault bounded borderland basin	A–CS10
10.	Ciezkowice			3–30+				Lenticular	MS, T	T, H	Base of slope, confined	A
11.	Claymore Sst	0–470		1–3	15	10		Blocky, sheet	MS, T	Tfg, H	Basin, confined, tectonically active	A–HC
12.	Cow Head Gp*		> 100	< 40	37	15		Sheet/lenticular	MB	D, T	Carbonate slope apron	A–M
13.	Crater Lake			< 1	< 5			Wedge	Ms, T, D	Rf, D, Tfg, H	Base of slope apron	Mod
14.	Denbigh Grits*	150						Channel	MS, Tcg	Tfg, H	Canyon/feeder channel	A
15.	Dothan Sst		3–85					Channel	MS, Tcg	T, H	Fan channel	A
16.	Exuma Sound			5–7	120	25		Broad lens	MB		Basin	Mod–M
17.	Franklinian Basin			< 30	~ 30	~ 3		Tabular, elongate	MS, D, T	MB, T, H	Elongate trough	A
18.	Franklinian Basin			< 270	250			Tabular, wedge	MB	T, H, D	Elongate trough	A–M
19.	Frigg Field*		80	4–20				Lobe sheets	MS, T	Tfg, H	Stacked lobes — mound (close to channel mouth)	A–HC
20.	Goldenville Fm*		10–30	< 6	15			Lenticular/channel	MS, T	Tfg	Channel fills, channel complexes, mid fan	A
21.	Gordo Megabed*			< 40	17	11.5	6	Sheet/lenticular	MB	T	Small tectonic basin	A–M
22.	Gran Canon Fm			< 20				Lenticular/wedge	MB, MS	D, S, T, V	Volcanic slope apron	A–V
23.	Gres d'Annot Sst*	250	50	4.5	10	6	12	Infill sheet	MS	H, Tfg	Structurally controlled small basin	A–CS8
24.	Gryphon Field*	0–120			10	8		Complex, mounded	MS	H, Ij	Basin	A–HC
25.	Guweyza Fm	250		< 20				Sheet/lenticular		T, H	Slope apron wedge	A
26.	Hakrim Fm*			< 15	> 1			Channel	MB	Tcg, SW	Proximal fan-delta, back arc basin	A–M
27.	Hareelv Fm	50			5	0.4	< 0.005	Channel	MS	Tfg, H, Ij	Slope gullies — lobes	A
28.	Heimdal Fm*	100–120	10–80					Sheet	MS	H	Distal fan	A–HC
29.	Herodotus Megabed*			8–20	> 450	100	400	Sheet	MB	Tfg, H	Basin plain	Mod–M

(continued on next page)

Table 1 (*continued*)

Appendix reference	Example	Thickness (m)			Geometry (km)				Massive sand facies association (dominant)	Associated facies (encasing) (dominant)	Depositional setting (inferred)	Category
		Body	Unit	Bed	Length	Width	Volume (km^3)	Shape				
30.	Kopervik Sst*							Elongate, lensoid	MS	T, H	Small basin, axial fan	A–HC
31.	Kowmung Volcs		< 40					Tabular	MS	RF, D, T	Volcanic apron	A–V
32.	Ksiaz Fm			1–5				Tabular	MS, D, Tcg	D, Tcg	Fan-delta, toe zone	A
33.	Maesan Fan-Delta*	~ 100		< 6	2–3		1–2	Sheet/chute/lobe	MS, T	T, SW	Fan-delta fault slope-apron	A–CS6
34.	Marnosa Arenacea*			9–16	120	30	48	Sheet	MB	T, H	Tectonic elongate basin	A–M
35.	Marlim Field	30–100		< 12				Tabular	MS	T, H	Slope	A–HC
36.	Matilija Sst*		40–60	2–7		100–200		Tabular	MS, T	T, H	Fault-bounded borderland basin	A–CS7
37.	Merrions Tuff			< 2				Sheet/lenticular	MS, T	T, V	Fan channel	A–V
38.	Misaki Fm*			4–6+				Lenticular	MS, T, H	T, H	Forearc basin	A–V
39.	Mississippi Fan*	400	10–20	< 10	20	10		Broad lens	MS, T	Tfg	Fan lobe (channel mouth)	Mod
40.	Mississippi Fan*			29				Sheet/wedge	MB	T	Mid-fan	Mod–M
41.	Modelo Fm		< 30					Lenticular	MS, T	Tfg, H	Fan	A
42.	M. Sacro Fm		25	1–4				Wedge	MS, Tcg+fg	T	Fan (gravelly) in structural basin	A
43.	Mullock Bay Fm		15					Channel	MS, Tcg	Tfg, H	Lobe	A
44.	Namorado Sst	80						Mounded	MS	Tfg, H	Slope	A–HC
45.	Nicosia Fm*	50		< 6	> 1	> 0.2		Lenticular	MS, T	H, SW	Fan-delta, toe zone	A
46.	Numidian: Contrada*	40–45	1–20	1–8	> 3	0.5		Channel	MS	H, Tfg, Ij	Slope channels, external foredeep basin	A–CS5
47.	Numidian: Pollina*	250–500	> 25	1–12	> 25(?)	1–3	~	Broad channel	MS, T, D	Tfg, H, S, Ij	Slope channels, external foredeep basin	A–CS4
48.	Numidian: Finale*	40–80		< 4.2	> 10(?)	0.15–0.3	0.13	Channel	MS, Tcg, D	Tfg, H, S	Slope channels, external foredeep basin	A–CS3
49.	Numidian: Gagliano		~ 50					Channel(?)	MS		?Channel, active margin	A–HC
50.	Otadai Fm*			1–10	30	5		Tabular, lens	MS, T	T	Mel-fan channel/lobe	A
51.	Pigafetta Basin*			4–11				Wedge, sheet	MS, D, T, S	T, H	Mid-ocean basin plain	A–V
52.	Pinas		> 30					Wedge	MS	Tcg	Active margin	A
53.	Quebrada de los Lajas*	~ 100		< 10				Lenticular	MS, Tcg, D	T	Tectonically active basin	A
54.	Reitano Flysch*			~ 20				Wedge, sheet	MB	T	Active margin basin	A–M
55.	Rhuddnant Grits*			< 2				Tabular	MS, T	Tfg+cg	Basin, active margin	A
56.	Roncal Megabed			30–100	75	12			MB	T	Small tectonic basin	A–M
57.	S. Mauro Fm			< 5				Tabular	MS, T	Tcg+fg	Lobes in piggy-back basin	A
58.	Scaglia Rossa*			5–6		3–5		Broad lens	MS	S, D, T, P	Small basin	A
59.	Seathwaite Fell Fm*	< 200		< 30				Sheet	MS, T	T	Caldera lake	A–V
60.	Seathwaite Fell Fm*	< 200	< 30	< 20				Ponded sheet	MS, D, T	T	Caldera lake	A–V

61.	Shelter's Cove Fm		30–100	> 1.5				MS, Tcg	T, H	Fan channel	A
62.	Singing Creek Fm		< 30	< 2				MS, Tcg+fg	Tfg	Fan channel	A
63.	Sivas Volcaniclastics			< 15	~ 0.5	Tabular, apron		MS, T	D, Tfg, H	Tectonically active slope	A–V
64.	Skewi Fm			< 12	200	50		MB		Small basin	A–M
65.	Snowy R. Volcanics		< 25	2–15				MS, T	D, T, H	Active margin	A–V
66.	Sogneford Fm		5–35				Lenticular	MS	H	Faulted slope, structural depressions	A
67.	Tabernas Fan*		30–75	1–6	5		Channel	MS, T	Tfg, H	Channels–lobe system	A
68.	Tesnus Fm	~ 30	3–8	< 2.5				MS, T, S	T, H	Axial channel, fan	A
69.	Umegase Fm*		35	1–14	27	3	Lenticular sheet	MS, T	T	Forearc basin	A–CS1
70.	Urbanian Sst*	30–300	> 50	1–10	35	2–3	8	Elongate	MS, T	T, H, Ij	Elongate active basin	A–CS2

[a] See Fig. 1 for locations; source references for each are given in Appendix A. Facies abbreviations: MS, massive sand; MB, megabed; T, turbidite (cg coarse-grained, mg medium-grained, fg fine-grained); D, debrite; H, hemipelagite; P, pelagite; RF, rock fall; S, slide/slump; Ij, injected sand; V, volcaniclastics; SW, shallow water facies. Categories: A, ancient; Mod, modern; CS1, case study 1; M, megabed; HC, hydrocarbon-bearing; V, volcaniclastic; see Appendix A for references; *examined by authors this study.

clastic lithologies, from both the surface and subsurface. Nine examples are known hydrocarbon reservoirs and 12 are megabeds that include a massive sand unit. The rest are surface outcrops that represent deposition of massive sands in a wide range of tectonic settings.

Some of the principal characteristics of these 70 examples are given in Table 1 and their locations shown on Fig. 1. We have considered, but do not report upon, many more examples from both modern and ancient deep-water successions that did not fit our criteria of massive sand (i.e. originally >4 m of essentially structureless sand). The database is still growing and we already know of a further 10–15 examples for which we had insufficient information at the time of going to press. Of these 70 examples, we have studied ten in detail (Case Studies 1–10) and examined a further 25 in the field. The ten case studies include three from the Oligo-Miocene Numidian Flysch of Sicily, three late Mesozoic and Paleogene examples from California, two Pliocene examples from the Far east (Japan and Korea), one Eocene foreland basin example from southern France, and one example from the Miocene Marnosa Arenecea Formation of the Italian Apennines.

For each example given and for each case study documented, we have considered systematically the following aspects (Stow et al., 1995): location, age and formation; geological stetting, structure and stratigraphy; lateral extent and basin geometry; vertical succession and mesosequences; sediment facies and petrography; and an interpretation of the depositional setting, sandstone geometry, facies and processes, and reservoir characteristics. Summary information is given below for each of the case studies examined in detail. The data presented in the rest of the paper is drawn first from these and then from all available sources.

1.3.1. Case study 1: Umegase formation (Ito, 1992; Ito & Katsura, 1992)

The Kazusa Group, as much as 3000 m thick, is the fill of a Plio-Pleistocene forearc basin (Kazusa forearc basin). This group is represented by a series of marine environments ranging from deep-sea basin-plain, through submarine fan and slope, to shallow seas, which retrograded during the Pliocene to the earliest Pleistocene and then prograded. The Umegase Formation (up to 530 m thick) represents the middle portion of the Kazusa Group and is characterised generally by thick- to very thick-bedded turbidite sands deposited to a small slope-fan environment. Individual sand bodies can be traced for over 27 km and have a width of 3 km. The Umegase Formation intercalates with the Higashihigasa Formation of submarine canyon-fill sediments about 220 m thick and the overlying Awakura Formation of shelf to shelf edge

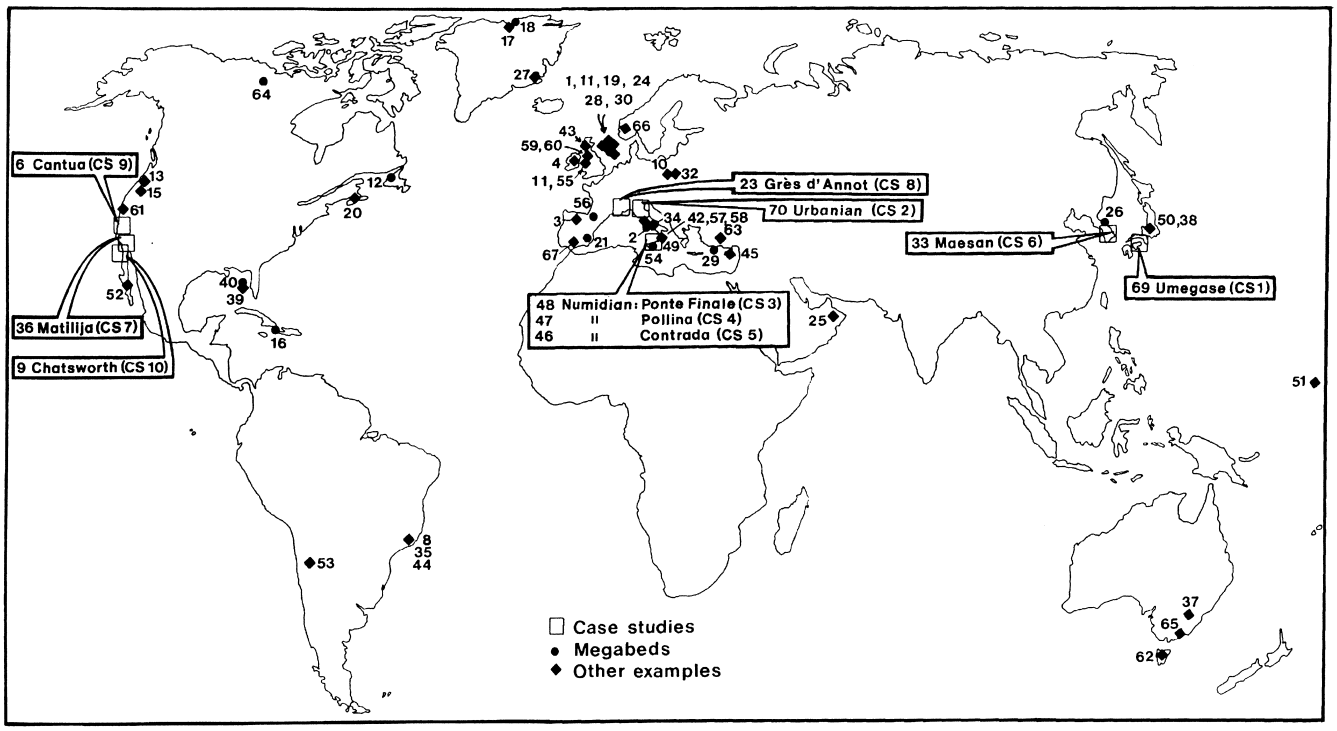

Fig. 1. Map showing location of all examples of deep-water massive sands used in this study. Numbers refer to details given in Table 1. Ten detailed case studies highlighted.

sediments about 190 m thick. Furthermore, the Umegase formation is underlain by middle to lower fan sediments of the Otadai Formation about 540 m thick. The very thick-bedded sands have a lenticular shape, an overall convex-up geometry and occur in units averaging sand–shale ratios of 9.5:1.

1.3.2. Case study 2: Urbanian sandstone (Ardanese et al., 1987)

The Urbanian sandstone is part of the late Miocene (Tortonian) Marnosa Arenecea Formation of central Italy, that accumulated in a narrow, elongate, minor basin of the Adriatic foredeep sedimentary domain. The massive sandstone complex ranges from 30 to 300 m in thickness, encased in a normal turbidite succession, and extends some 35 km through the Urbanian–Serraspinosa linked basin system. The sands are believed to have been structurally confined to the more axial region of the 8–10 km wide basins. Very thick bedded structureless sandstones form >85% of the succession (typical sand–shale ratios of 9:1) and have a very immature petrographic signature indicating derivation from a mainly alpine source, with axial transport along the foredeep basin system. There is strong evidence for post-depositional liquefaction and partial remobilisation of the sands.

1.3.3. Case studies 3, 4 and 5: Numidian Flysch Formation (Hoyez, 1989; Johansson et al., 1998; Parise & Beaudoin, 1986; Parise, Beaudoin & Fries, 1999; Roure, Howell, Muller & Moretti, 1990)

The Numidian Flysch Formation of northern Sicily forms part of a much more extensive E–W trending external foredeep basin system bordering the northern margin of Africa as it collided progressively with Europe. Although difficult to measure because of structural complexities, the Numidian Flysch may be as much as 2 km thick in parts of Sicily. Within this typical fine-grained turbiditic association, there are distinct intervals of sandstone and conglomerate facies (sand–shale ratios of 9.5:1–7.5:1), that are interpreted as representing the fill of sinuous to meandering slope channels.

At *Ponte Finale* (*CS3*), there is a prominent headland and steep sandstone cliffs exposed for a distance of some 2 km. Three separate channel complexes can be recognised, ranging from 25 to 65 m in thickness and from 150 to 300 m in width. They have scoured, erosive and stepped margins, with internal erosion and channel nesting evident. Immediately inland, near *Pollina* (*CS4*), there are several further outcrops along the flanks of dry river valleys and on upstanding peaks and ridges. All sections studied show channel-like geometries, individual complexes being 1–3 km wide, 250–

300 m deep and probably at least 10–20 km long. Major slump units are associated with the deeply erosive margins, and channel migration is evident over several km laterally and a few hundreds of metres upsection. Still further inland, parts of the internal Numidian are well exposed as high sandstone bluffs encased in mudstone facies. At *Contrada di Romana* (*CS5*), near the town of Nicosia, the sandstone complex is 40–45 m thick, 450–500 m long and forms part of the overturned limb of a thrust nappe fold. The sands occur in very thick, very structureless units with extensive water-escape features. Here as well as at other Numidian Flysch outcrops, there is much evidence of post-depositional sandstone remobilisation and injection into the surrounding lithologies.

1.3.4. Case study 6: Maesan fan-delta (Chough, Choe & Hwang, 1993)

A series of fan-deltas were deposited during the Miocene adjacent to the Yangsan Fault system bordering the Pohang basin in SE Korea. The Maesan complex is interpreted as a steep-faced fan-delta characterised by coarse-grained facies deposited on high-gradient slopes. Very thick structureless sands occur as part of a generally coarser grained assemblage deposited as avalanche sheets, slide-slump complexes, chute-lobe bodies and in shallow ephemeral channels. Sand:shale ratios are high to very high (5:1–9.5:1).

1.3.5. Case study 7: Matilija sandstone (Link, 1975; Link & Welton, 1982)

Eocene rocks of the Santa Ynez Mountains in Southern California record two major regressive events, the Juncal-Matilija followed by the Cozy Dell–Coldwater–Sespe sequences. The Matilija Sandstone is interpreted as representing a deep-water succession through a transition zone to a shallow water succession, totalling a minimum thickness of 720 m. The sediments are thought to represent a deep-sea fan complex through to shallow marine deltaic and coastal plain facies representing a single cycle of deposition. Reconstruction of the basin based on outcrop studies indicates it must have been tens of kilometres wide and at least 100–200 km long. The original structural setting for the deposition of the Matilija Sandstones is thought to be within a Eocene fault-bounded borderland setting. The Matilija sands occur in units with sand–shale ratios averaging around 9.5:1 and are enveloped by thick marine shales of the Juncal and Cozy Dell Formation.

1.3.6. Case study 8: Annot sandstone (Elliott et al., 1985; Stanley, Palmer & Dill, 1978)

The lower Oligocene Annot sands in Alpes de Provence, southern France, were deposited in a foreland basin setting, and outcrop over an area of some 60 km^2. The maximum vertical thickness at Annot is 250 m, which comprises over 90% thick, amalgamated, non-graded and poorly graded coarse to pebbly sandstones, with associated thin-bedded sandstone to mudstone turbidites (sand–shale ratios $>9{:}1$). The whole succession both erodes into and onlaps onto underlying hemipelagic basinal marls. Supply to the basin was broadly from the south and sandstone geometry was closely controlled by the basin topography.

1.3.7. Case study 9: Cantua sandstone (Graham & Berry, 1979; Nilsen, Dibble & Simoni, 1974)

The Cantua Sandstone forms one of the main members of the Paleogene Lodo Formation in the western San Joaquin Valley, California. It ranges up to 1375 m in thickness and extends over an area 35×15 km (surface and subsurface). It is dominated by thick and very thick bedded sandstones associated with more normal turbidites and encased in basinal mudstones. The massive sands display a broadly tabular geometry, although individual sheets comprise an overlapping series of flattened lenticular units that are amalgamated into thicker tabular bodies of probable basinal extent. Sand–shale ratios generally exceed 9.5:1. The depositional setting was a structurally-controlled, small Borderland-type basin in a tectonically active area.

1.3.8. Case study 10: Chatsworth formation (Link, Squires & Colburn, 1981)

The Late Cretaceous Chatsworth Formation is part of the Central Transverse Ranges in central California. The formation is over 1.8 km thick and comprises around 90% amalgamated, thick bedded sandstone units, that are up to 60 m or more in thickness, with the bed thicknesses ranging from 0.5 to 6 m. The sands are thought to have been deposited very rapidly in a restricted, actively subsiding, Borderland basin situated on an epicontinental site. The lateral extent of the main sandstone complexes is estimated at around 40 km. Individual units as well as individual beds are broadly lenticular but, due to bed thickness compensation, they impart an overall tabular geometry.

2. Facies and facies characteristics

2.1. The massive sandstone facies association (MSFA)

In some examples studied, the DWMS body was deposited in or onto a uniform fine-grained hemipelagic succession — these are isolated DWMSs. More commonly, however, the DWMS occurs in association with a closely related range of mainly coarse-grained resedimented facies that we call the Massive Sandstone Facies Association (MSFA) (Fig. 2). The MSFA thus comprises the following facies:

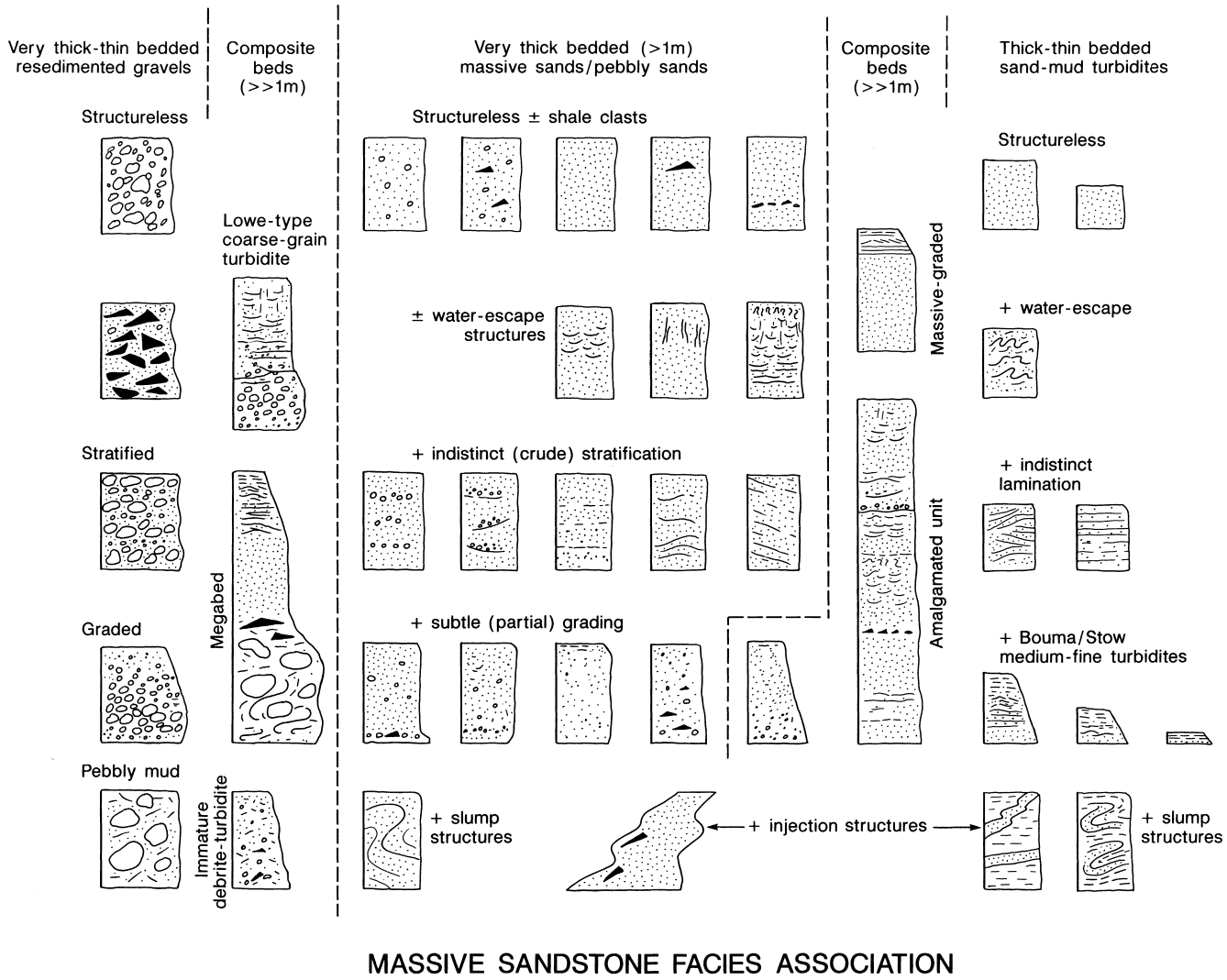

Fig. 2. Massive sandstone facies association, with schematic indication of key features.

very thick-bedded (>1 m) structureless sands/pebbly sand (<10% pebbles) (DWMS) sensu stricto, central facies panel in Fig. 2)

- completely structureless, with or without shale clasts
- structureless, but with water-escape features
- apparently structureless, but with an indistinct (crude) parallel or cross-stratification
- mainly structureless beds, that show partial grading, including normal or reverse at the base, normal at the top, or very subtle coarse-tail grading
- apparently structureless, but with faint evidence of slump contortions
- structureless, with evidence of injection;

very thick to thin-bedded gravels and pebbly sands (>10% pebbles) (lefthand column, Fig. 2)

- completely structureless
- composed dominantly of shale clasts
- crudely stratified (parallel or cross-stratification)
- graded (normal, reverse or both)
- pebbly muds;

thick to thin-bedded sand-mud units (turbidites) (right-hand panel, Fig. 2)

- structureless sand
- structureless sands, with water escape features
- indistinctly laminated sands (parallel, wavy, cross)
- graded sand-mud units with Bouma sequences
- graded silt-mud units with Stow sequences
- slump-structured sand-mud deposits
- thin sand iinjections into mud units;

very thick Composite beds (≫1 m) (columns as marked, Fig. 2)

- graded/ungraded/reverse graded gravels and sands (±water escape features)

- disorganised or immature graded gravel-sand-mud beds
- megabeds, grading from boulders/gravels/pebbly muds to sands to muds
- massive sands with graded turbidite tops
- amalgamated massive sand units.

Examples of the true DWMS facies are illustrated in Fig. 3. Certain specific characteristics are discussed below, with data drawn from the full range of examples studied.

2.2. Bed thickness and bed boundaries

The MSFA in general shows thick and very thick beds of coarse-grained facies, with relatively minor intervals of thin-bedded turbidites and hemipelagites. We have not tried to estimate an *average* bed thickness from the incomplete data provided in the literature, but can obtain a better idea of maximum bed thicknesses for the massive sands (Fig. 4, Table 1).

These data show a broad peak of beds between 2 and 8 m thick, with a tail of others up to 16 m thick and then more isolated examples up to 20 m and a maximum recorded of 30 m for a single identifiable bed. For a number of examples we are unable to distinguish true beds from maximum thicknesses given for what are most probably amalgamated units. These are typically over 15 m and range up to 100 m in thickness. In some cases we only have a value for the entire sand body, which is commonly in excess of 100 m. Recorded thicknesses of megabeds, typically debrite-turbidite couplets, are scattered from about 10 m (usually taken as the lower limit for a megabed) up to 100 m. Massive sand portions of these megabeds range from 5 m up to some at 25 m.

A complete range of bed boundaries is observed, both top and base of the massive sands. They vary from distinct and sharp to completely gradational amalgamation contacts. In addition, basal contacts may be slightly to deeply erosive, cutting down from a few tens of centimetres to a few tens of metres into the underlying sands or muds. More irregular and wavy contacts, at either top or base, are most likely due to post-depositional remobilisation causing loading and/or injection.

2.3. Texture and composition

There are no very definitive textural or compositional attributes that can be said to hold for massive sands in general, although certain interesting characteristics can be observed (Figs. 5 and 6). Mean grain size and maximum (non-shale) clast size of the range of beds within the MSFA both show an increase with bed thickness up to about 2.5 m thick beds. The truly thick massive sand beds, however, tend to show a more uniform mean grain size (fine-medium sand) and an apparently quite different trend of maximum (non-shale) clast size with bed thickness. Clast size remains relatively small even for the thickest beds.

As would be expected, the sorting parameter decreases with increasing grain size (hence bed thickness) for most of the MSFA beds. However, the very thick massive sands are typically poorly to moderately poorly sorted whatever the bed thickness.

From these data, based on the somewhat limited results of our ten case studies, it would appear that massive sands are generally finer-grained and with smaller maximum (non-shale) clast sizes that would be expected for such thick beds. One explanation for this would be that the 'apparent' bed thickness is the result of amalgamation of several thinner (1–3 m thick) beds. In other words, the grain size is more typical of a 2 m thick bed than a 10 m thick bed. There is some supporting evidence for this in terms of water-escape sequences. An alternative explanation is that massive sands are deposited by a somewhat different and more uniform process than the range of MSFA facies. Speculatively, this might, for example, be by continuous aggradation/collapse fall-out from an HDT that experiences an hydraulic jump due to a topographic obstacle or gradient change.

The composition of massive sands depends ultimately on the nature of the source area, both original and transitional. Our studies reveal a complete range, from $>95\%$ quartz (e.g. the Numidian Flysch), to $>80\%$ lithic (volcanic) grains (e.g. the Umegase Formation), to highly feldspathic (30–50%) sandstones (e.g. the Californian examples) (Fig. 7). In Fig. 5, we have tentatively shown our depositional setting Types I–IV with respect to their QFL composition. Although we do not propose that these relationships are strictly observed, they do offer a general guide.

2.4. Shale clasts

One important characteristic of massive sands, and MSFA beds in general, is the presence of shale clasts (Fig. 8). These vary considerably in terms of size, shape, abundance and, position in the bed. Careful study has revealed eleven different genetic types each of which yields significant information about the nature and deposition of the host bed (Johansson & Stow, 1995). They include:

1. top-bed rip-down clasts formed by post-depositional fluidisation of the sand, possible lateral movement and a stoping, loading or rip-down of the overlying shale
2. base-bed raft-type clasts formed by high energy ero-

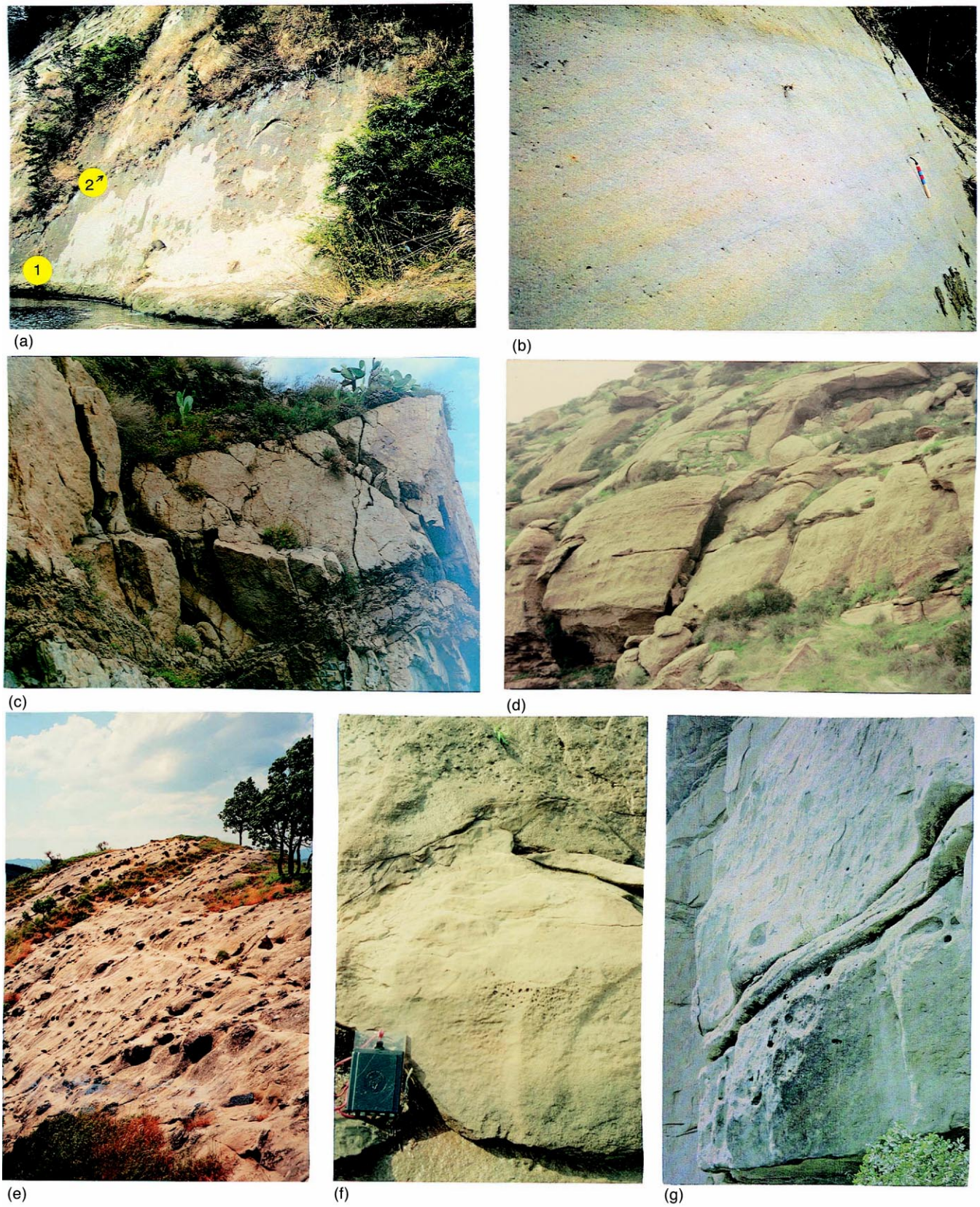

Fig. 3. Photographs showing selected attributes of massive sandstone facies. All beds are right way up. (a) Part of 14 m thick massive sandstone (Bed 1), Umegase Formation, Japan. Bed 2 is a thin overlying turbidite sand bed. (b) Detail from Bed 1, shown in (a), showing completely structureless aspect. (Photos a and b courtesy of Makoto Ito). (c) Part of 4 m thick massive sandstone bed erosive into (or amalgamated with) an irregular shale-clast zone, Numidian Flysch, Ponte Finale, Sicily. (d) View shows >20 m of massive sandstone unit, in fact comprising 1–5 m thick beds separated by amalgamation surfaces, Chatsworth Formation, California. (e) Part of very thick (>100 m) massive sandstone body with rare indication of bed contacts and numerous carbonate concretions, Urbanian Sandstone, Italy. (f) Detail of massive sandstone with irregular pebble-rich zone, Matilija Sandstone, California. (g) Detail near base of Annot Sandstone, SE France, showing amalgamation horizon and irregular shale clasts.

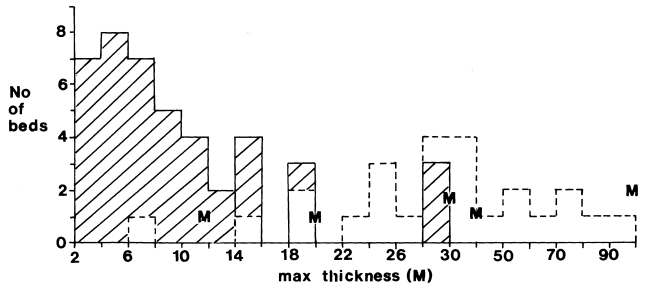

Fig. 4. Spectrum of bed/unit thickness for massive sands based on data from the 70 examples used in this study. Note that thicknesses are shown in 2 m bands below 30 m and in 10 m bands above 30 m.

sive rip-up of the underlying shales in the final stages of sand deposition

3. base-bed flame-type clasts formed by loading of the sand into softer unconsolidated mud causing flame injection and break off
4. isolated floating clasts emplaced either by deposition from an HDT at any point along its flow path by a process of continuous aggradation, or by deposition from a SDF by plug freezing
5. clustered floating clasts emplaced as in no. 4 but more typical of the more distal parts of HDT flow subject to gradient change or topographic obstacles
6. clustered amalgamation clasts formed by the erosional break-up of a thin intervening shale layer between successive sand beds
7. chaotic shale clast conglomerate representing a true debris flow deposit, perhaps resulting from channel margin collapse or headward slumping
8. ordered stratified/cross-stratified clasts indicating normal particle behaviour of clasts and sand grains passing through a period of traction at the base of an HDT
9. ordered scour-lag clasts formed by erosion, infilling and possible tractional winnowing at the base of an HDT, probably more likely in collapse fall-out deposition
10. dispersed graded clasts indicating normal particle behaviour and coarse-tail grading as a result of collapse fall-out from a turbulent HDT
11. isolated sand-ripped clasts formed by post-depositional injection of sand into an adjacent shale formation and forcible rip-off along the sand dyke walls.

Although we can identify these 11 different types and be confident in our interpretation of their mode of origin, we have not yet gathered sufficient data to fully utilise them as a tool in understanding or predicting massive sand types and depositional settings. However, our preliminary speculations suggest the following relationship between clast type, transport–depositional process and transport distance:

- types 2 and 9 indicate high energy erosion (proximal)
- types 3 and 6 indicate lower energy erosion (distal)
- types 4 and 5 indicate HDT or SDF deposition by aggradation in more proximal and more distal settings, respectively
- types 8 and 10 indicate tractional and suspension collapse deposition respectively from an HDT
- type 7 indicates SDF deposition
- types 1 and 11 indicate post-depositional liquefaction with or without major lateral movement and injection.

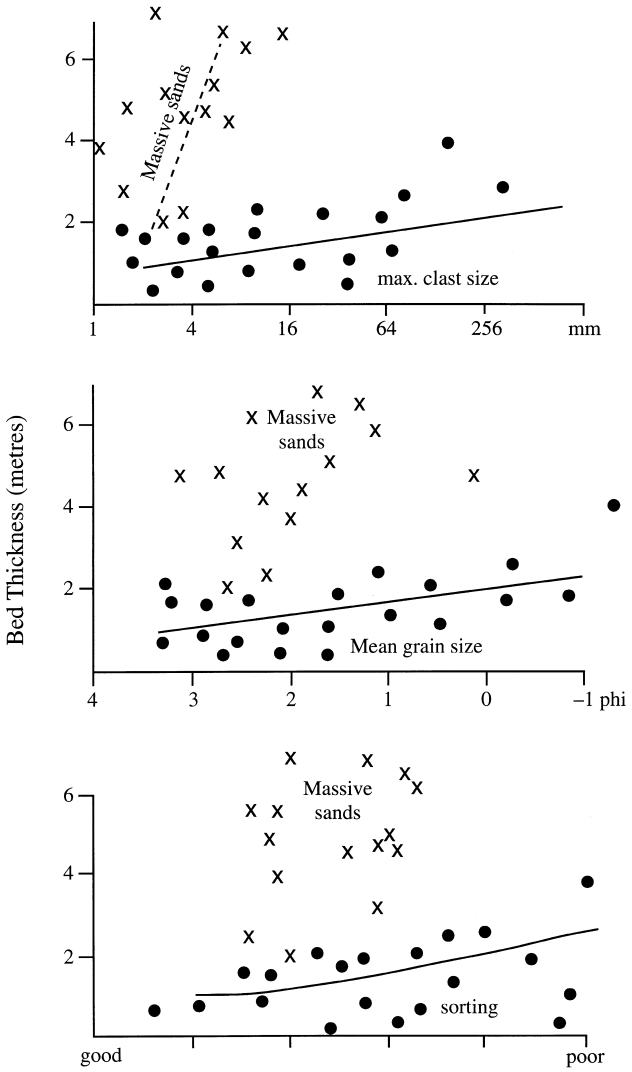

Fig. 5. Textural characteristics of massive sands (dashed lines, crosses) and other members of the massive sandstone facies association (trends shown by solid lines, solid circles), based on data from the ten detailed case studies.

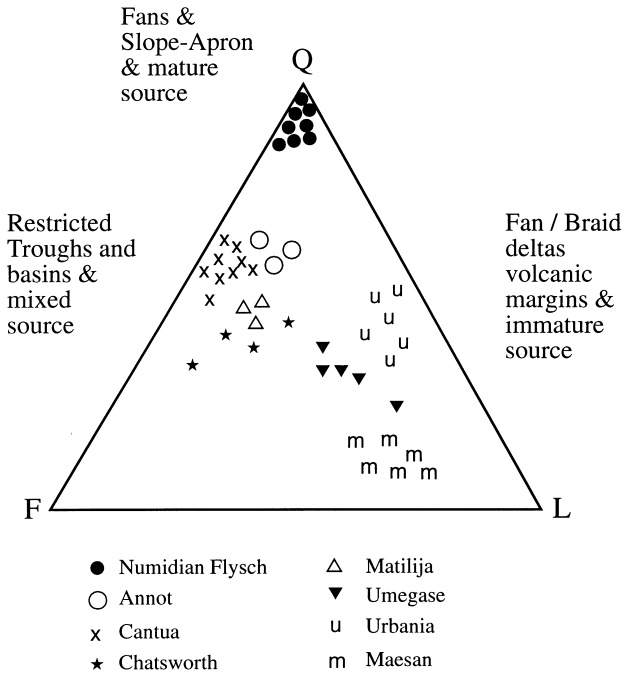

Fig. 6. Compositional characteristics of massive sands shown on a Quartz–Feldspar–Lithics (QFL) plot based on data from examples reported by other workers and the case studies used in this study. Different compositions are characteristic of different depositional settings.

2.5. Water-escape features

Water-escape structures of various types (dishes, pillars, etc) are common features of many of the massive sands examined for this study. As they are one of the very few features that may yield diagnostic information, a careful record was kept of their nature and presence.

We recognise an ideal sequence of water-escape structures (Fig. 9). This comprises, from top to base:

- zone vi — characterised by contorted laminae, in some cases with burst-through features, large or small-scale sand volcanoes etc
- zone v — characterised by vertical pipes (pillars) with poorly developed intervening dishes
- zone iv — characterised by abundant narrow width dishes, with some vertical pipes
- zone iii — characterised by broad width dishes and rare intervening pipes
- zone ii — characterised by indistinct, subparallel consolidation laminae
- zone i — which is entirely structureless.

This is similar to the sequences recognised by previous workers (e.g. Lowe & Lopiccolo, 1974) but somewhat refined and extended. The full sequence is rarely present and repeated partial sequences may indicate amalgamation of thinner beds (1–3 m thick) into thicker massive sand units. Detailed measurement of dish wavelength (width) and amplitude (depth) confirms the Zi–Zvi sequence noted, as well as the probable amal-

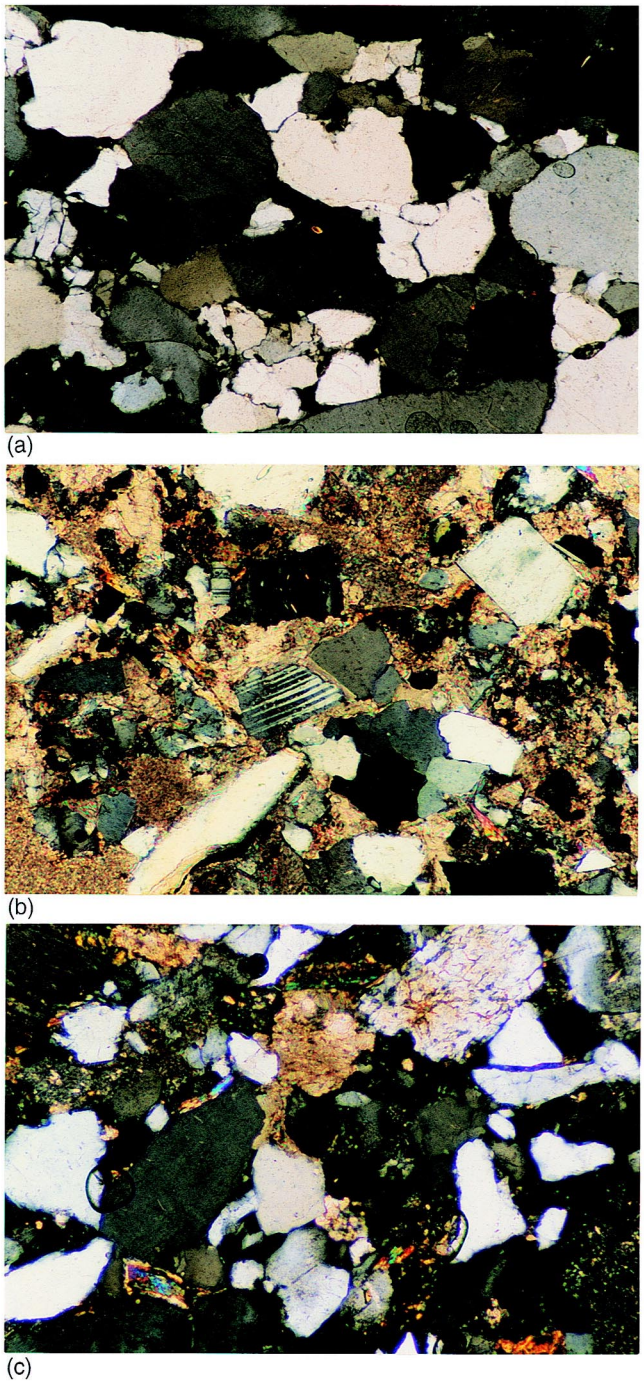

Fig. 7. Selected thin section micrographs from massive sandstone facies: width of view 2.5 mm; cross-polarised light. (a) Numidian Flysch, Ponte Finale, Sicily — highly quartz-rich. (b) Urbanian Sandstone, central Italy — quartzo-feldspathic with carbonate cement. (c) Annot Sandstone, SE France — quartz rich with feldspar and lithics.

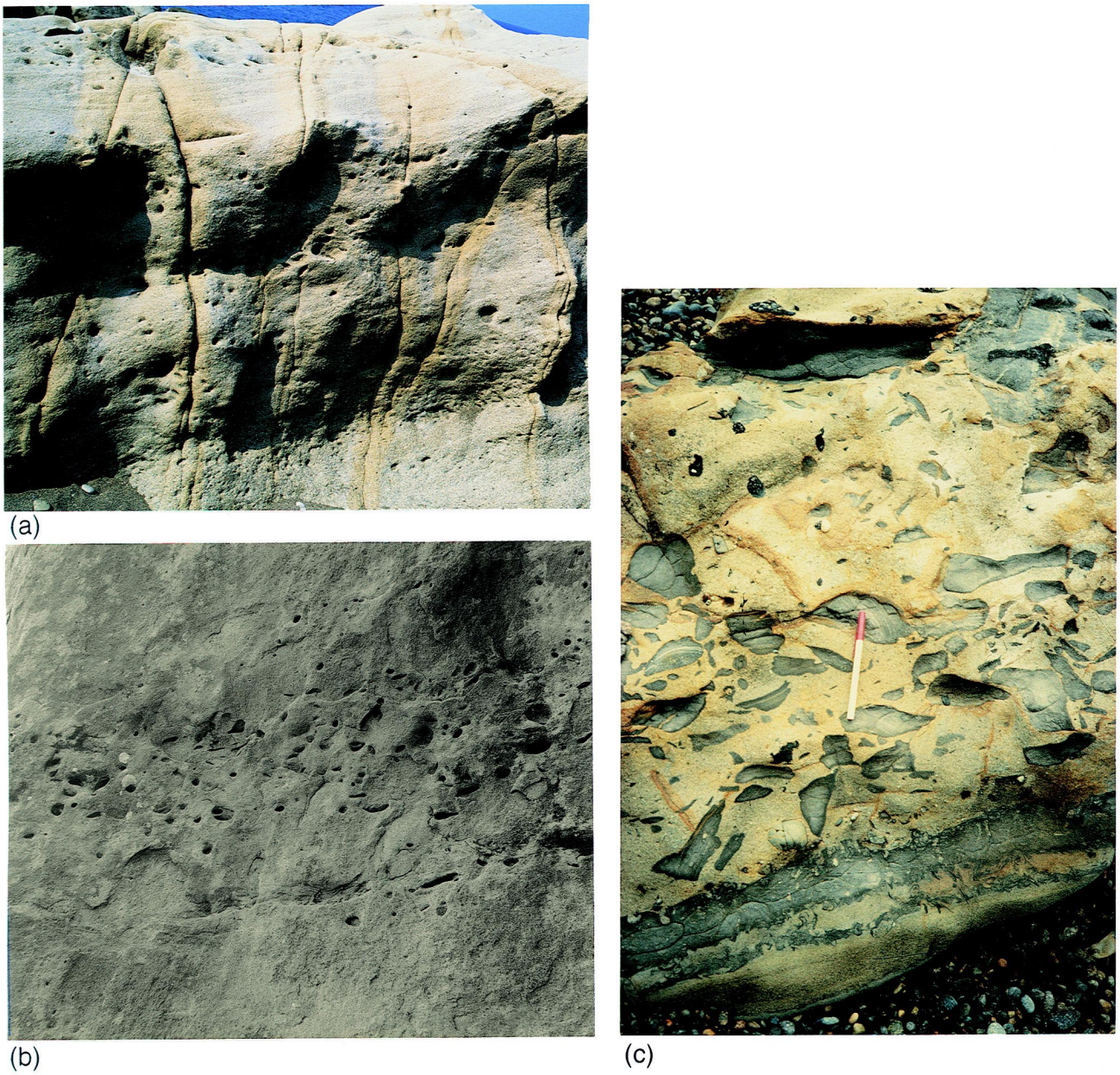

Fig. 8. Photographs of selected shale clast types in massive sand facies. (a) Dispersed graded shale clasts in Reitano Megabed, N Sicily. (b) Clustered floating clasts/clustered amalgamation clasts, Annot, SE France. (c) Chaotic shale-clast conglomerate, Point Lobos, California (photo courtesy of Bryan Cronin).

gamation of thinner beds. These results are reported in detail by Braakenburg (1994).

The interpretation of water escape structures and their vertical arrangement does not find full agreement in the literature. Lowe and LoPiccolo (1974) infer the prior existence of semi-permeable lamination followed by gradual dewatering of "internal" pore fluids, whereas Allen (1982) infers forceful injection of "external" fluids, and an impermeable capping to the sandstone horizon.

Our study suggests problems with both models in that (1) we see very little evidence for lamination even in parts of massive sand beds immediately adjacent to zones of water-escape structures; and (2) there are rarely any impermeable caps to the sand beds. We would therefore favour Allen's stoping mechanism but suggest that the pore fluids are internally derived. Furthermore, the succession of fluid-escape sequences observed in amalgamated units would suggest *rapid* dewatering immediately after deposition rather than the gradual dewatering proposed in previous models. However, we do note that recent experimental work has shown that forceful injection of external fluids from the basal glide plane of a fast moving sandy deb-

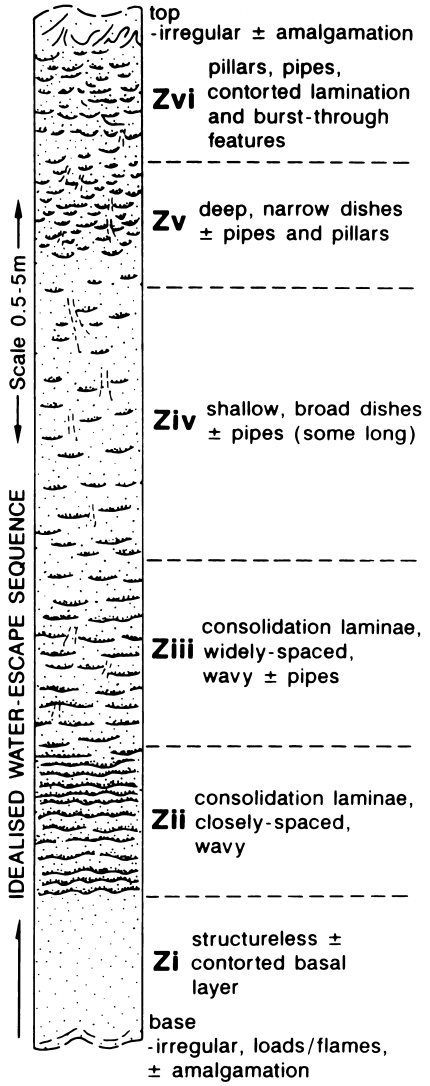

Fig. 9. Idealised vertical sequence of water-escape structures (Zi–Zvi) in massive sands.

ris flow can cause water escape features to be developed in the sandy debrite deposit (Shanmugam, personal communication). The likely form of these water-escape features requires further study.

Our preferred explanation for the complete sequence of water-escape structure is that it begins to form during rapid deposition through the basal active layer of an HDT. While the layer is thin and the volume of fluid therefore small there is little impediment to upwards fluid escape and the bed remains structureless (Zi). As the rate of deposition increases (and/or some tractional laminae begins to form) fluid is trapped and begins to move laterally forming wavy, bed-parallel, consolidation laminae that are intermittently breached (Zii). By this time deposition of the bed is probably complete. The lower parts are still relatively starved of fluid, and form broad, shallow dishes with widely spaced breaches (Ziii). As the rate and magnitude of fluid escape increases progressively higher in the bed, breaks between dishes are more closely spaced, forming narrow, strongly concave-up dishes and intervening pipe structures (Ziv). Within the upper limits of the bed, fluid escape pressure might exceed the effective weight of the overlying sediment (dependent on depositional rate) with related sediment fluidisation and the formation of multiple pipes and sheet dewatering structures (Zv). This is capped by a zone of intense sediment disruption (especially obvious where prior lamination exists), including contorted lamination and surface water escape features e.g. sand volcanoes (Zvi).

The presence of water-escape features in massive sands, therefore, yields the following formation:

1. the sand was deposited rapidly from an HDT through an active basal layer of hindered settling (deposition from an SDF is also possible)
2. partial or complete sequences indicate depositional units (beds) and amalgamation of beds where a succession of sequences occurs
3. the sand has not been extensively fluidised and remobilised or injected.

The absence of water-escape features poses more of a problem:

1. they do not form readily in coarse-grained sediments (i.e. gravels and pebbly sands)
2. lateral variation in type, amount and presence of water-escape structures is the norm within any one bed or unit, but the reason for this is not fully understood
3. their complete absence from some sections may be related to final depositional mechanisms from an HDT, rate of sediment supply to and through the basal layer, to deposition from an SDF, or to some other combination of factors.

Clearly, more work is required on this aspect of massive sands.

2.6. Other features

A number of processes may operate following primary deposition and initial dewatering of massive sands. These may serve to significantly alter the original nature of the deposit and, in some cases, to make an originally organised/structured sand become structureless. We therefore outline these processes and their resulting features before discussing DWMS deposition.

2.6.1. Erosion, reworking and dewatering

Erosion of part of the massive sand by the same (autoerosion) or a subsequent HDT/SDF can occur

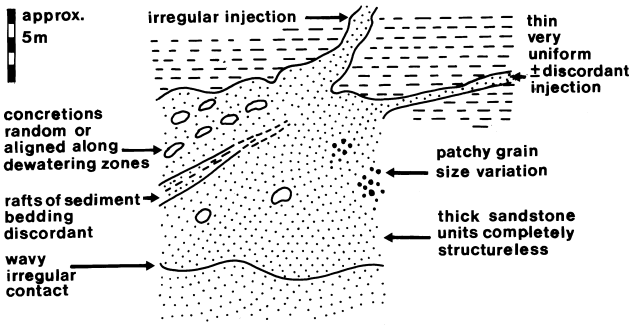

Fig. 10. Internal features in massive sand bodies that indicate partial post-depositional liquefaction and remobilistation. This is a schematic figure illustrating features found in several of the DWMS examples studied.

and is believed to be common. Normal erosive scours may then be observed in the deposit although the evidence may be largely removed by amalgamation. Undercutting and erosion of the channel margins by confined flows can lead to slumping and the incorporation of shale clasts into the flow. Reworking of the upper part of an earlier deposited sand by a subsequent non-depositing turbidity current or by some kind of bottom current (contour current, storm-induced current, deep surface-current, etc) will result in current-induced bedforms. Gravel waves, and waves, dunes and ripples are all observed on the surface of deep-water deposits at the present day. Such features are expressed by tractional structures (cross-stratification etc) in a preserved deposit.

2.6.2. Bioturbation

Bioturbation is not common in MSFAs, although where thin interbeds of fine-grained turbidites and hemipelagites occur then minor bioturbation may be evident. Massive sand successions that pass upwards to more shallow-water deposits will typically show a concomitant upward increase in bioturbation. In some instances a thick shallow-water sand body (e.g. a Gilbert micro-delta foresettled sand) may become thoroughly bioturbated and so lose most of its original internal structure. Mottling and ghost burrows will normally remain in evidence.

2.6.3. Liquefaction/remobilisation

There are a number of features within a massive sandstone facies association that indicate partial liquefaction and remobilisation of at least parts of the succession have taken place (Figs. 10 and 11). These include:

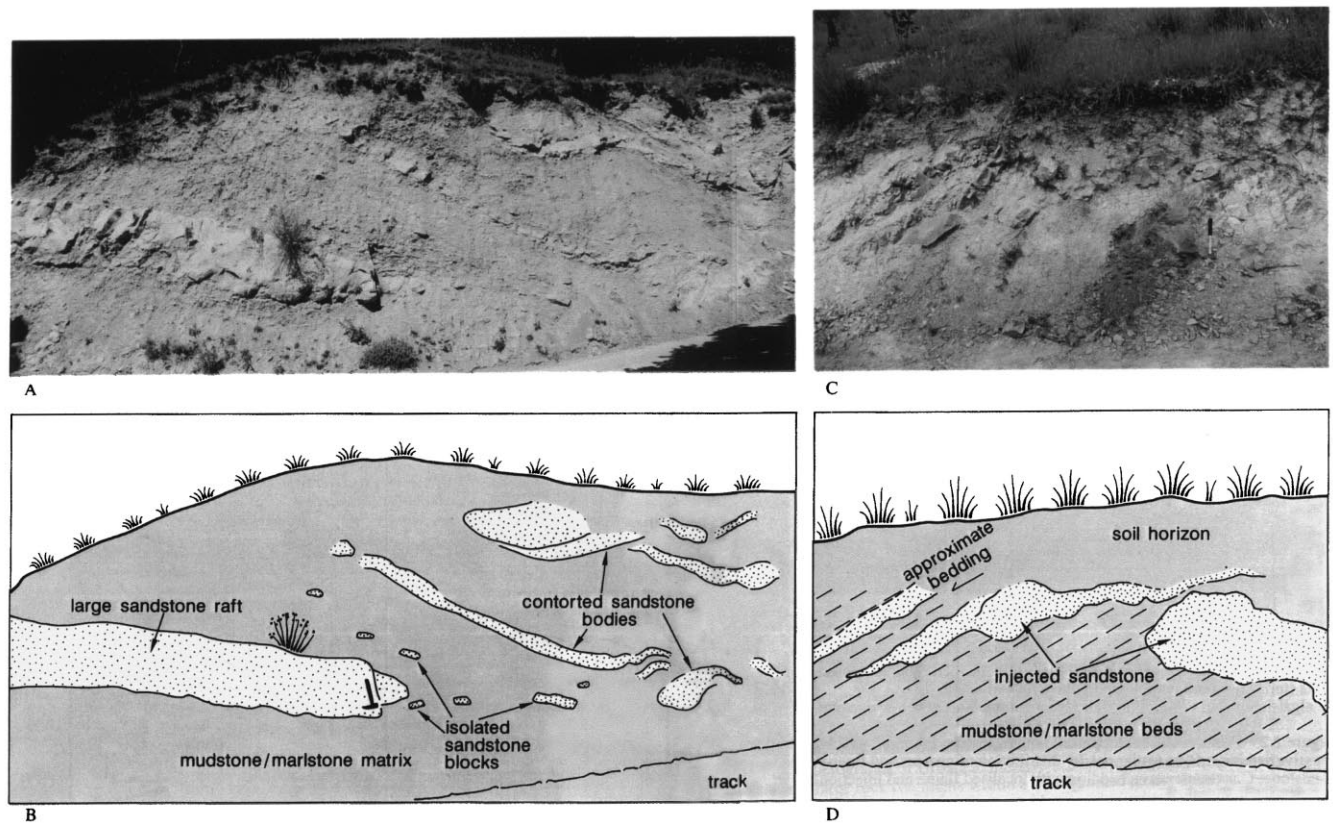

Fig. 11. Photographs of injection features in massive sands, together with line drawing interpretation. Urbanian Sandstone, near Urbania, central Italy.

- irregular patchiness of coarse and medium-grained sand on a decimetric scale
- discontinuous bedding horizons
- bed bases that are extremely irregular or wavy and show local injection from the base upwards
- unusual cross-cutting relationships of true and apparent bedding planes/laminated units
- common dewatering partings or joints
- general homogeneity of thick tracts of sand with an absence even of water-escape features and bedding
- concretions that are arranged either randomly or in alignments indicative of dewatering pathways;

Complete liquefaction of the sands and whole-scale remobilisation is evident where:

- sand dykes and sills intrude into the surrounding sediment
- the top surface of the sand body is highly irregular and extends part way up fault planes
- the margins of the sand body are unusually steep and/or irregular but without showing evidence of downcutting channel erosion.

Thick bodies of poorly consolidated sands encased in a fine-grained turbidite/hemipelagite succession are very subject to liquefaction and remobilisation as a result of seismic shock and seismic pumping of fluids through fault and joint systems. Many of the features listed therefore will be common in such deposits, i.e. especially Type II and Type III (channel) deposits.

3. Process of transport and deposition

Based on our own detailed observations of massive sand characteristics, and with reference to the growing body of literature that pertains more directly to the deposition of coarse-gained material by resedimentation processes (Allen, 1991; Carter, 1975; Hein, 1982; Kneller & Branney, 1995; Nemec, 1990; Postma, 1984; Postma, Nemec & Kleinspehn, 1988; Shanmugam & Moiola, 1995, 1997; Stow, 1994), we propose the following synthesis of massive sand origin.

The emplacement of massive sands and other members of the massive sand facies association can be considered in three stages: (1) initiation and proximal processes, (2) long distance transport processes, and (3) depositional mechanisms. These are summarised in Fig. 12 and discussed in the following.

3.1. Initiation and proximal processes

Subaerial alluvial fans and coarse-grained deltas that feed directly onto a submarine slope can initiate a number of downslope resedimentation processes on the submarine portion of the fan delta/braid delta system.

Rock fall (*RF*) *or avalanche* involves the sudden displacement of solitary grains and boulders or loose particle assemblages that fall, bounce or roll downslope for several tens or hundreds of metres before coming to rest.

Creep (*CR*) involves slow integranular frictional sliding as a result of load-induced stress (i.e. the downslope weight of sediment). Both continuous and intermittent creep are widespread slope processes and, at high ratios of shear stress to shear strength, creep deformation may accelerate rapidly to creep rupture and thus act as a precursor to slide failure.

Sliding and slumping (*SL*) are more or less synonymous terms that describe downslope displacement of a semi-consolidated sediment mass along a basal shear place while retaining some internal (bedding) coherence. Sliding emphasizes the lateral displacement along either simple translational or slightly rotational shear planes with little internal disturbance, whereas slumping emphasizes the internal disturbance and folded shear planes.

The complexity of slide features on modern slopes has been amply demonstrated by recent studies (Barnes & Lewis, 1991; Lee, 1989), which clearly shows the gradation that exists in nature between slide, debris flow and turbidity current processes and products. A *flow-slide* is the term given to this kind of transitional process from sliding to debris flow.

Sediment instability is very widespread on all submarine slopes, not just those of fan deltas and braid deltas, and is affected by numerous interacting variables including: (1) the slope angle; (2) high rates of sedimentation, leading to high water content and low shear strength; (3) repeated cyclic stress, commonly caused by seismicity but also influenced by oceanographic factors such as currents and internal waves; (4) high primary productivity and/or bottom water anoxicity, both leading to high organic carbon content in the sediment; and (5) generation of gas in the sediment due to clathrate decomposition and organic matter decay.

Whereas the failure of unstable muddly sediments caused by seismic shock may lead to a coherent slide-slump mass and this, in turn, evolve into a muddy debris flow, unstable sandy sediments are likely to undergo liquefaction. The resulting flow-side of sandy material may move largely by grain flow and fluidised flow processes, and come to rest very rapidly through the loss of the grain support mechanism (Lowe, 1976; Middleton & Hampton, 1976). Alternatively, it may ignite by a process of water entrapment beneath the moving flow and transform into an aquaplaning sandy debris flow (Mohrig, Whipple, Hondozo, Ellis & Parker, 1998; Shanmugam, 2000).

The only other process that can initiate resedimentation of coarse sandy material are pyroclastic flow into

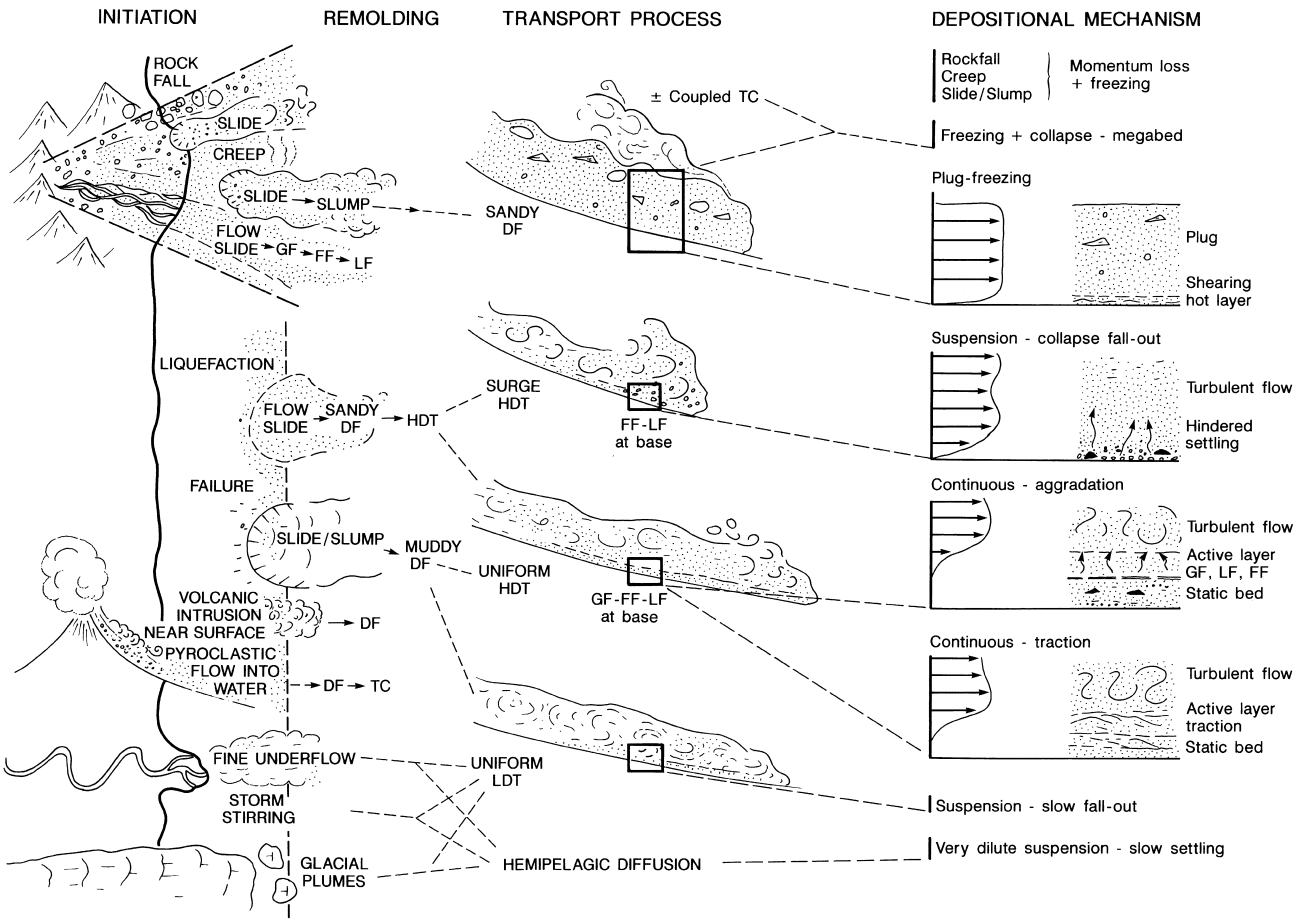

Fig. 12. Initiation, transport processes and depositional mechanisms involved in the origin of massive sands (modified from Stow et al. (1996)).

a standing body of water and volcanic intrusion just beneath, and breaking through, the wet sediment surface of a submarine slope. Both processes can lead to chaotic debris flows and subsequent turbidity currents.

3.2. Long-distance transport processes

The only sediment-gravity processes capable of transporting large volumes of coarse-gained material over relatively long distances (i.e. > few kilometres) are debris flows and turbidity currents. For the deposition of massive sands, sandy debris flows (SDF) and high concentration turbidity currents (HDT) are the important processes.

Debris flows (*DF*) are highly concentrated, highly viscous, sediment dispersions that possess a yield strength and display plastic flow behaviour (Hampton, 1972). They are widespread on both subaerial and subaqueous slopes, and may be either granular (also known as grain flows) or cohesive in nature. Subaqueous debris flows appear to move in one of two ways: (1) as slow moving, slurry-like or glacier-like, laminar flows that advance down slopes in excess of only 0.5°, either continuously or intermittently; and (2) as fast moving, semi-rigid plugs or rafts or material that aquaplane over a low-friction basal shearing layer. In both cases, debris flows move when the critical yield strength is exceeded and deformation (flow) begins in a basal zone of highest shear stress. Transformation from a slow moving to fast moving flow occurs as a result of high pore pressure build up in the basal zone (Gee, Masson, Watts & Allen, 1999; Masson, Kenyon & Weaver, 1996; Masson, van Niel & Weaver, 1997) and by water entrapment beneath the overlying flow-plug (Shanmugam, 2000). We call this process, flow ignition, by analogy with turbidity currents. It is these high-velocity debris flows that are likely to have long run-out distances (i.e. > 100 km) and to emplace thick units of massive sands in deep water. Deposition occurs by loss of water from the basal layer and downward thickening of the plug until the entire mass freezes. Flow margin freezing may also occur and result in the construction of debris levees.

It appears most likely that natural debris flows dis-

play a wide range of rheological properties, being more or less cohesive-plastic, viscous-fluid and granular-collisional in behaviour (Pickering, Hiscott & Hein, 1989). The clast support mechanisms would also vary, including a combination of buoyancy, frictional strength, matrix strength, elevated pore pressures of the matrix, and dispersive pressure. Pickering et al. (1989) also discuss the possibility of some very large flows being turbulent in part.

Turbidity currents (*TC*) are a type of density current or gravity current (Simpson, 1982) in which the denser fluid is a relatively dilute suspension of sediment. Depending on the manner in which the flow is initiated and on subsequent sediment supply, two main types of turbidity current can be identified: (1) relatively short-lived surge-type flows, and (2) relatively long-lived steady- or uniform-type flows. Surge-type flows can evolve into uniform flows by a process known as flow ignition. Furthermore each of these types may be either high density (HDT) or low-density (LDT) turbidity currents, with complete gradation between the two end members and with potential evolution from one to the other during a single flow event. Both types develop into composite flows at some stage of their evolution, comprising a lower stratified flow, from which deposition occurs, and an upper turbulent flow. Shanmugam (1996) considers the decoupled parts of such flows as an HDT over an SDF.

In all turbidity currents the sediment-support mechanism which keeps the sediment particles in suspension is provided primarily by the upward component of fluid turbulence, which is mainly sustained by friction at the boundary between the flow and both the floor and the ambient fluid. As the gravitational force acting on the excess density of suspended sediment propels the flow, so a state of autosuspension or flow self-maintenance is achieved (Southard & Mackintosh, 1981). It is therefore possible for a turbidity current to travel over long distances without appreciable erosion or deposition as long as the slope remains constant. The development of a lower stratified layer will probably lead quite rapidly to deposition via collapse or freezing, although it may continue to be pulled along a considerable distance by fluid drag at its upper surface.

There are several combinations of temporal and spatial velocity change in a turbidity current, largely dependent on change of bottom gradient and of sediment concentration due to fallout. These will influence the style of deposit that results (i.e. structureless/laminated, graded/ungraded) (Kneller & Branney, 1995).

3.3. Depositional mechanisms

Although long distance transport may be restricted to SDF and HDT processes, the basal zones of such flows typically show a much modified behaviour involving gliding, shearing, grain flow, fluidised flow and liquefied flow. At times they may show considerable erosive capability, whereas at other times the basal zone experiences net sediment loss and deposition occurs.

There are four principal depositional mechanisms that result in the accumulation of massive sands.

1. *Freezing* of the shearing layer beneath an SDF plug as it advances slowly downslope, following a period of rapid movement by aquaplaning where this has occurred. This preserves the nature of the SDF intact.
2. *Collapse fall-out* from the turbulent flow of an HDT as it loses momentum, becomes unstable and rapidly deposits. Sediment may pass briefly through a basal zone of hindered settling where modified grain flow, fluidised flow and liquefied flow support mechanisms operate. This is typical beneath a short-lived surge type HDT, but may also occur from a uniform HDT where it encounters an abrupt change of gradient.
3. *Continuous aggradation* beneath a sustained steady or near-steady HDT with sediment passing through an active basal layer of hindered settling (also known as a traction carpet, decoupled turbidity current, SDF layer). Grain flow, fluidised flow and liquefied flow processes may all operate and, together with the top of the static bed, pass slowly up through the overriding fully turbulent flow as deposition proceeds. Deposition will continue as long as the downward grain flux to the static bed is balanced by sediment supply from the HDT.
4. *Continuous traction* beneath a sustained steady or near-steady HDT. Bed-load traction will occur as opposed to grain flow-fluidised flow where the rate of sediment supplied to the basal zone is not so excessive as to swamp the tractional process. This is not normally the case so that large-scale cross-stratification (dune cross-bedding) is rare in turbidites and DWMS beds.

Transformation between any of these four mechanisms appears possible so that any single deposition (massive sand bed or unit) may involve SDF and HDT transport processes with final deposition via one or several of the mechanisms described. Furthermore, the tops of massive sands may be capped by slow fall-out from suspension (a fine-grained turbidite). Megabeds most likely result from freezing followed by collapse fall-out of a coupled debris flow-turbidity current. The largest megabeds may also involve sliding at the base. It is therefore unhelpful to consider and unlikely in nature that DWMS beds are the result of a single process (see the recent debate in the literature: Shanmugam, 2000).

Ultimate deposition will occur when the transporting process loses forward/downslope momentum and the grain support mechanism collapses. For the proximal processes (rockfall, creep, slides, debris flow, flow-slides) this generally occurs relatively close (<1 km) to the point of initiation, typically on the slope of the fan/braid delta or slope-apron system. Flow dilution and transformation via ingestion of ambient fluid may occur, as well as fluid entrapment beneath the flow, resulting in a longer-lived debris flow or turbidity current.

Deposition from one of these more long distance transport processes typically occurs: (i) where there is a marked change in slope gradient, (ii) where the flow meets a major topographic obstacle, (iii) where a confined flow leaves its channel and expands laterally, and (iv) as a result of flow stripping, flow spillage and flow lofting from the main body of the flow. Continuous deposition and aggradation may occur at any point along the path of the flow.

4. Geometry and sequences

4.1. Sand body geometry

Massive sands occur as part of a broader facies association (MSFA) within a three-dimensional sand body or sand complex. Sand/shale ratios within these bodies are everywhere in excess of 5:1 and more normally from 7:1 to >9:1. The body itself is more or less distinct and may not show good connectivity with other related sand/gravel systems.

Based on as many examples as possible for which we were able to obtain size parameters (see Table 1) we have plotted length against width and illustrate the probable two-dimensional geometries of different sand body types (Fig. 13). Broadly speaking there are four main types.

1. *Small-scale sand bodies* are associated with fan- or braid-delta systems. There comprise narrow chutes, broader ephemeral channels, debris flow tongues,

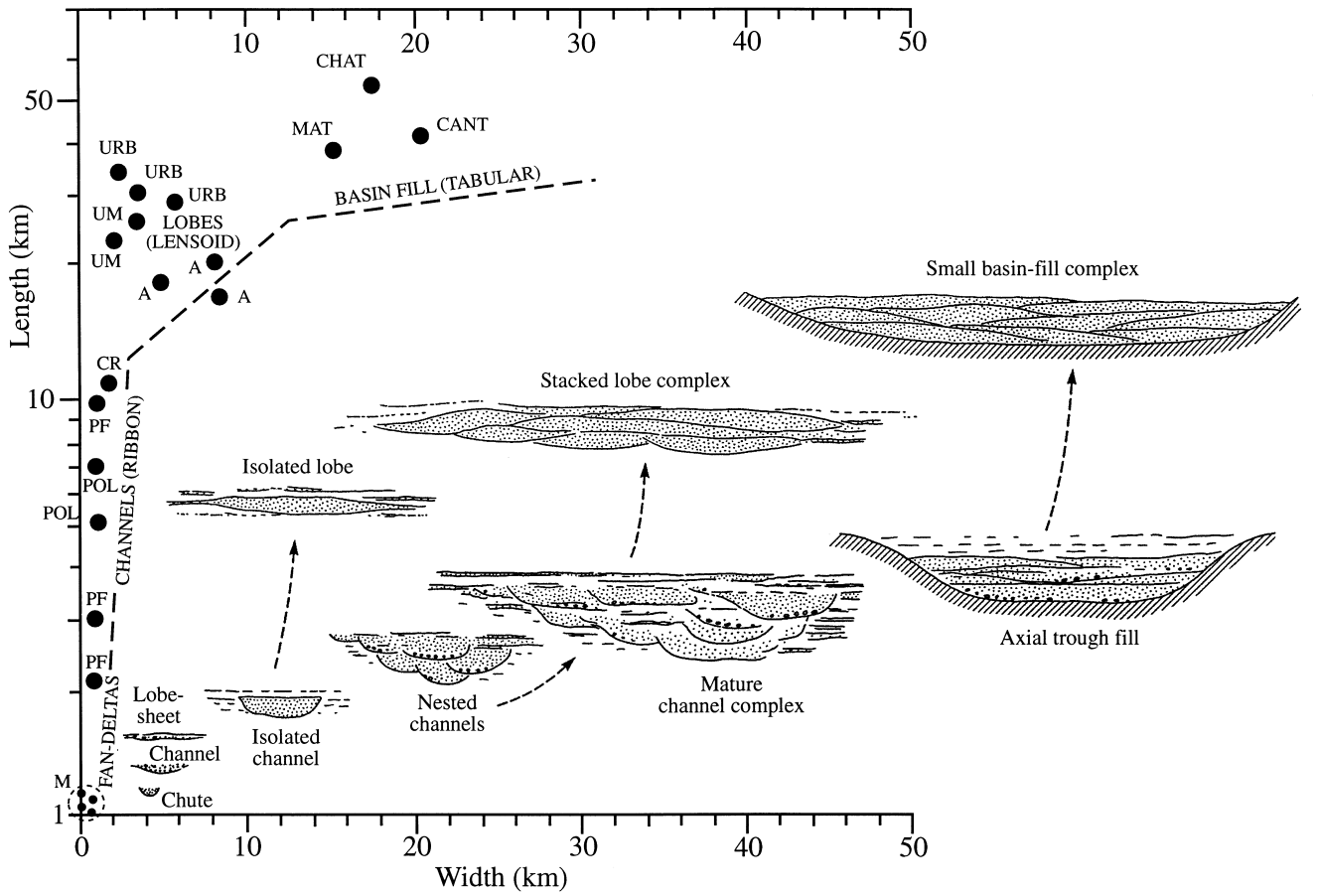

Fig. 13. Massive sand body geometry. Length to width ratio for 21 examples of massive sand bodies examined in the case study areas, and schematic representation in two dimensions of sand body geometry for the different systems identified. Case studies: CHAT, Chatsworth formation; CANT, Cantua sandstone; MAT, Matilija sandstone; URB, Urbanian sandstone; UM, Umegase formation; A, Annot sandstone; CR, Contrada di Romani; POL, Pollina; PF, Ponte Finale; M, Maesan.

lobe-sheets and flow-slides with length–width ratios ranging from 3:1 to 1:2. The total area of any one body rarely exceeds 0.25 km^2 and the thickness is generally < 50 m. Connectivity with other coarse-grained facies and bodies within the fan/braid-delta is typically good so that the whole system may be up to 500 m or more in thickness with a fan radius of 2–5 km.

2. *Channel, tongue or ribbon-like sand bodies* may occur as isolated, nested and mature systems. They are elongate bodies with length–width ratios of between 5:1 and 15:1 as far as can be determined from preserved portions of ancient successions. Based on modern channels we would expect ratios up to 50:1 or 100:1 to be commonplace, though what proportion of the channel length would contain the MSFA is not known. Modern examples of debris flow tongues give length–width ratios of 10:1 to 50:1, somewhat less than for channels. Ancient systems preserve total areas up to 5 km^2 and thicknesses < 100 m for isolated channels, ranging up to 35 km^2 and < 500 m thick for mature (stacked) channel complexes. The degree of sinuosity is not well known, but we would speculate that isolated channels display low sinuosity, whereas mature channel complexes can show a high degree of meandering in their more distal reaches. Connectivity is poor for isolated channels but may be moderately good for mature channel complexes that are part of much larger fan systems. We should expect poor connectivity for isolated debris flow tongues.
3. *Lobate or lensoid sand bodies*, like the channels and debris flow tongues that feed them, may occur as isolated, clustered or stacked lobe complexes. As far as can be determined from the preserved record, length–width ratios range from 2:1 to 4:1. This appears to agree with studies of modern systems, although it is not always clear where a lobe ends and 'interlobe' sedimentation begins. Isolated lobes may be up to 8 km^2 in area and 100 m thick, whereas stacked lobe complexes can reach 50 km^2 and 500 m in thickness. Connectivities range from poor to good.
4. *Trough and basin sand bodies* are generally lensoid to tabular in shape. Structurally confined troughs may have a more channel-like geometry with length–width ratios of 5:1 to 10:1 and can reach several hundreds of metres (or more) in thickness. The (small) basins they feed have length–width ratios of between 3:1 and 1:2, areas up to and over 500 km^2 and thicknesses commonly between 1000 and 2000 m. Their internal architecture may be very similar to stacked lobe complexes, displaying broadly lensoid to tabular sand body geometries.

Where a trough/basin system has remained in deep water then it is likely to be encased in fine-grained sediment and show zero or low connectivity with other sand bodies. Repeated basin fill sand bodies may, however, be separated by only relatively thin shale horizons (i.e. tens of metres). Where basin fill is achieved through sand input, then the massive sand may pass upwards to a shallow-water coarse-grained succession with which connectivity will, of course, be very good.

4.2. Internal architecture and vertical sequences

The internal architecture of massive sand bodies refers to the lateral and vertical arrangement of individual beds and units within the body. In general terms it seems that the unit or bed geometry mirrors that of the whole body. Thus in lobes the individual beds are lensoid/lobate becoming more tabular or sheet like in the large lobes and basin systems. In channels they tend to be concave-downwards lensoid to erosive gully-shaped, becoming broader lensoid to tabular in the wide channel complexes and trough systems. Smaller scale versions of these shapes apply to the fan-delta sand bodies. Debris flow tongues are more likely to be convex upwards, except where they have travelled down as existing channel.

In the lobe and basin systems, we have further recognised a pattern of bed-to-bed thickness compensation by which successive beds compensate at least partly for the topographic expression of the underlying bed. This results in symmetrical sandstone compensation cycles or microsequences and, with bed-to-bed amalgamation, can lead to an apparent tabular geometry (e.g. Fig. 14).

We further speculate that within channel microsequences may exist, composed of "aggradational cycles" showing repeated blocky to fining-upwards patterns each of a few beds in thickness. As yet our evidence for this is very limited.

Vertical sequences of bed thickness/grain size variation, typically of a few tens of metres in thickness (mesosequences), are shown in Fig. 15. For fan-delta sand bodies they are generally irregular or blocky. Small (isolated) channel systems show blocky sequences whilst the isolated lobes they feed have blocky to broken blocky (i.e. with shale partings) sequences. The other channel, trough and basin systems all tend to show more or less blocky sequences, typically with partial (capping) or more complete fining-upward sequences and signatures broken by shale partings.

4.3. Modified geometry

Sand body geometry can be modified in several ways by syn- and post-depositional processes.

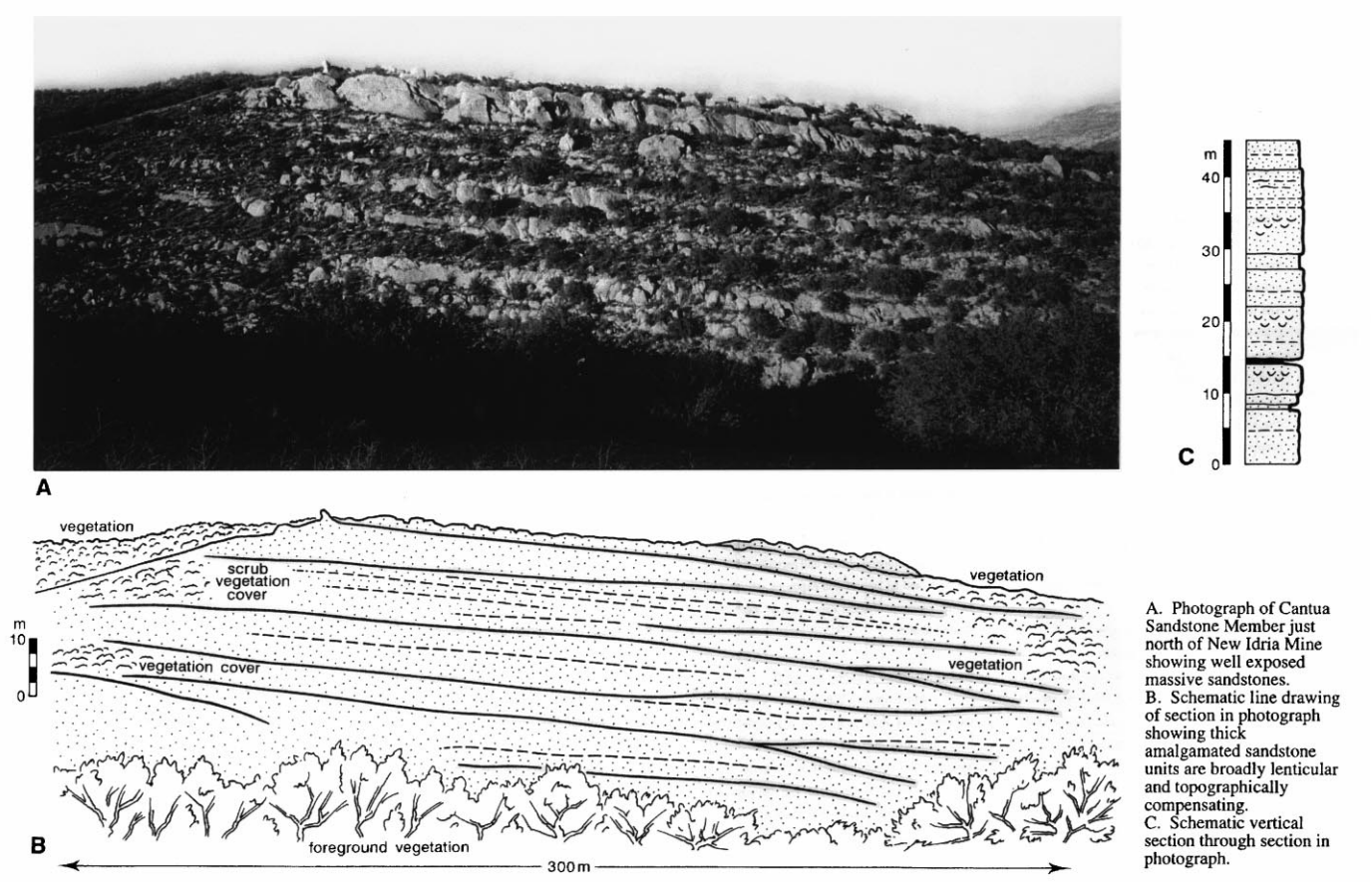

Fig. 14. Photograph showing thickness compensation cycles in massive sands, Cantua sandstone, central California.

1. Sand bodies that have been extensively remobilised and partly injected into the surrounding sediments may show more ragged irregular margins, with injection protrusions and oversteepened flanks.
2. Synsedimentary faulting at channel margins is commonplace as a result of differential compaction and loading. This can lead to stepped and oversteepened flanks.
3. Many of the systems studied were located in tectonically active settings. Feeder troughs and small basins may have one or more fault-controlled margins, creating more abrupt lateral contacts and/or locally thickened sections. Synsedimentary compression can lead to the development of structural topography that will serve to channel or deflect flows and/or localise deposition.
4. Extreme differential compaction will occur during burial between a massive sand body with >9:1 sand–shale ratio and the adjacent shale host, typically with a <1:9 sand–shale ratio. If we take, for example, a 100 m thick massive sand body channelled into hemipelagic shale, then 20% compaction of the sand and 60% compaction of the surrounding shale (very reasonable compaction figures), would lead to an 80 m thick sand adjacent and stratigraphically equivalent to 40 m thick shale unit. This would create the appearance of an oversteepened mould-like geometry.
5. Further and varied modifications, with dislocation between the sand body and encasing sediment, may result from late-stage processes of tectonic uplift and emplacement.

5. Depositional setting

5.1. Modern analogues

One major problem with the interprestion of deep-water massive sands has always been the lack of good modern analogues. Although our coverage and depth of study of present-day deep-water systems has improved dramatically in the last two decades, we still have incredible difficulty in adequately sampling coarse-grained unconsolidated sediments. Piston corers

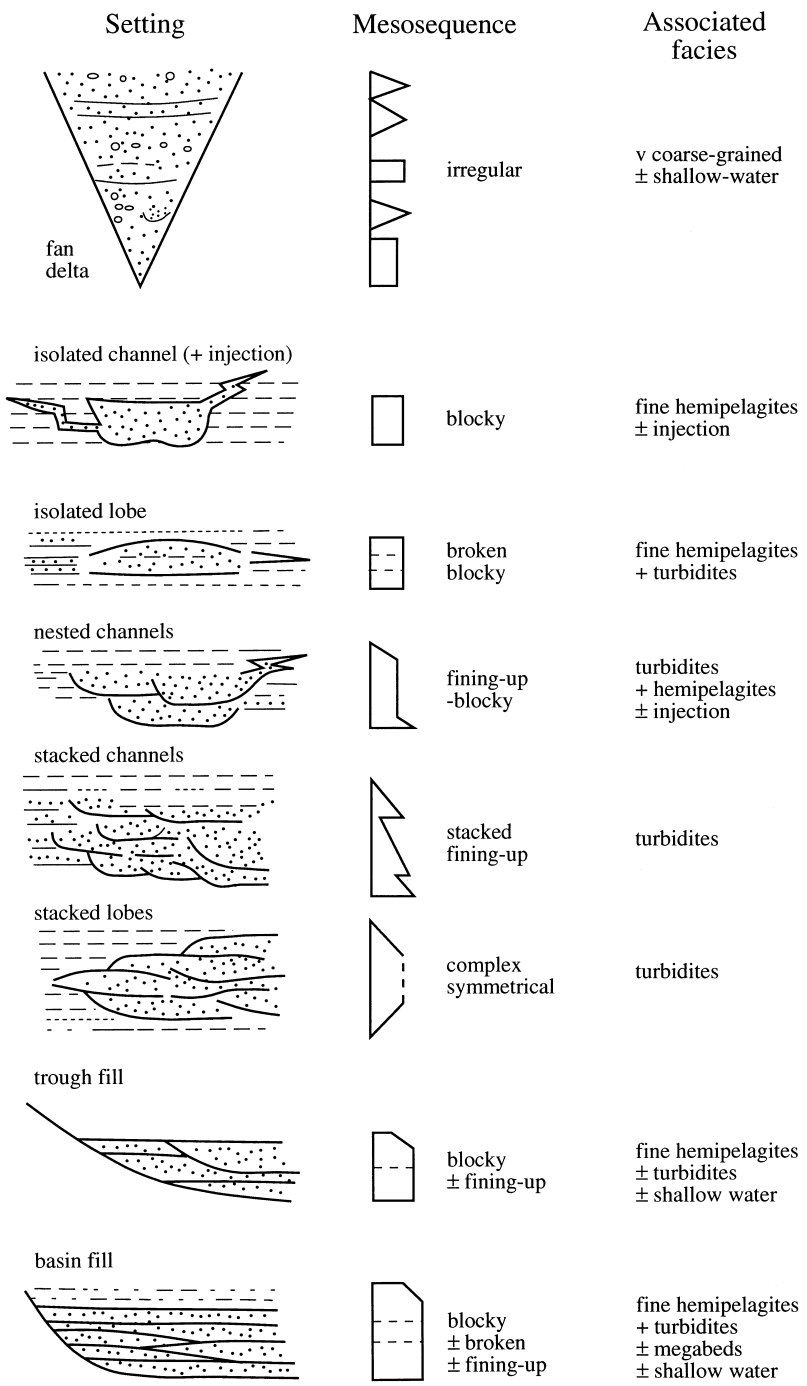

Fig. 15. Massive sand body mesosequences (i.e. vertical sequences of bed thickness and grain size over a few tens of metres) and associated facies found in different depositional settings. Lefthand column shows schematic views of depositional settings as marked — fan-delta in plan view, all others as cross sections.

and gravity corers bounce and bend on hard sandy substrates, our efforts to drill have mostly led to extensive wash-out and/or highly disturbed zones where we infer the presence of sands, and high-resolution deep-tow surveys still only give surficial maps of key areas of deep-sea floor. Nevertheless, we have accumulated some evidence and points in our search for present-day deep-water massive sands.

5.1.1. The Laurentian fan–Sohm abyssal plain

This has become one of the better known systems in which coarse-grained channel deposits are surrounded

by a mud-dominated turbidite fan (Hughes Clarke, Shor, Piper & Mayer, 1990; Piper, Normark & Stow, 1984; Stow, 1981). The 1929 Grand Banks earthquake led to major sliding and to the generation of a thick highly competent turbidity current. Gravel waves are observed over a distance of some 300 km down channel with wavelengths of the order of 25–80 m. Massive sands of up to about 10 m thick may occur in between the crests of gravel waves. Thick, well graded sand turbidites are deposited in the distal parts of the channel, over the lobes and become progressively thinner out across the Sohm Abyssal Plain.

5.1.2. The Hueneme fan (Piper, personal communication, 1992)

This is a small (5 km radius) sandy fan offshore western North America from which surface sampling and surveying has revealed probable thick (5–10 m ?) essentially structureless sands. Much thinner but very well sorted massive sands have been recovered from the neighbouring La Jolla Fan, offshore California, where the sands are derived directly from headward canyon erosion into the sandy offshore beach zone of La Jolla (Piper, 1970).

5.1.3. The Var Gilbert delta

Of late Pleistocene age, near Nice in southern France, this provides another example of a sand/gravel-rich source that is currently being eroded by muddy turbidity currents. A major slide in 1979 removed a portion of Nice airport together with a 20 km wide sandy shallow-water area and generated a highly competent turbidity current in the Var Canyon. Sandy deposits in excess of 1 m thick have been recovered, mostly with graded tops (Piper & Savoye, 1993).

5.1.4. The Orkdasfjord

In the Orkdasfjord, northern Norway, a sandy flowslide was dislodged by delta front/beach collapse and travelled some 20 km down the fjord axis to a depth of 500 m and deposited a massive sand body some 2–4 m thick. A similar event has been recorded from the Sandnessjøen fjord that deposited a sand body around 6 m thick (Bugge, 1983).

5.1.5. Mississippi fan

Drilling on the Mississippi fan (DSDP Leg 96, Bouma, Coleman et al., 1986; Stow et al., 1985) targeted mid-fan channel and terminal lobe settings of this muddy elongate fan. The channels were mud (and silty-mud) filled to a depth of 200 m, where drilling bottomed in a muddy gravel deposit. Rather than sand traps, the channels have acted, most recently, as very effective sand conduits dumping large volumes of sand on the channel-terminus lobes. Mostly, these are graded sand-mud turbidites separated by thinner silt-mud turbidites, but some massive graded sands may be up to 8–10 m thick. Drilling disturbance of the soft sands precludes setting confident limits on bed thickness.

5.1.6. Amazon fan

Drilling on the Amazon fan (ODP Leg 155) (Flood, Piper et al., 1995, 1997; Pirmez, Hiscott & Kronen, 1997) was still more extensive than for the Mississippi fan. Although typical of a mud-rich elongate fan, there is widespread distribution of thick sand units: (a) as laterally restricted channel-fill deposits that aggrade rapidly on the upper and middle fan; (b) as more laterally extensive systems below individual channel-levee complexes, formed as crevasse splay and channel mouth deposits; and (c) as depositional lobes on the lower fan. Each of these sand complexes can be 20– > 100 m thick, with sands commonly 0.1–4 m thick, and some beds > 10 m thick composed of medium to coarse-grained sand. Poor core recovery and coring disturbance once again make it difficult to ascertain whether or not the sands are truly massive, but good FMS records coupled with partial recovery suggest that some are. Shale clasts are particularly common in the thicker beds (> 1 m) of the channel fill and channel-levee basal sands, as well as in the very thick (> 3 m) lobe sheet sands.

5.2. The sandy contourite problem

As previous workers (Enjolras et al., 1986; Mutti et al., 1980, 1992) have speculated on the contourite origin of thick massive sand deposits, we have carefully examined the evidence from the modern record (Stow, Faugeres, Viana & Gonthier, 1998; Viana, Faugeres & Stow, 1998) and have drawn the following conclusions.

1. There is little evidence of thick sandy contouritic deposits in modern marine basins which could support the interpretation of ancient massive sand deposits as contourite. The thickest such deposits known at present are lenses of contourite sands (up to a few metres thick) that have mainly been inferred from subsurface data in the Gulf of Cadiz (Nelson, Baraza & Maldonado, 1993). However, limited core recovery means that their true nature and thickness is poorly known.
2. Other data on modern deep marine environments and associated deposits show that the contour currents may deposit and rework sand beds. However, these sandy contourites are restricted to particular morphologic and hydrodynamic settings which allow the enhancement of the current velocity, and for which an adequate sand supply is available. The extent and geometry of sandy contouritic deposits is highly variable: ribbons, irregular sheets, and cone-

like accumulations, ranging from <10 to >1000 km^2. The thickness of these beds range from a few cm to a few tens of cm. The sands are generally fine to medium-grained, poorly-sorted mixes of either siliciclastic material mixed with calcareous bioclasts (benthic to pelagic organisms from shallow to deep environments), or biogenic pelagic particles.

3. The process of deposition of sandy contourites involves mainly bedload transport; leading to specific bedforms (ripples, sediment waves, planar beds, ribbons), although the current structures are generally not very well preserved due to intense bioturbation. The reworking and winnowing of surficial deposits also occurs leading to relatively thin (<50 cm) lag deposits of structureless sands and gravels. Winnowing of turbidites appears to result in thin well-sorted (and commonly bioturbated) deposits.
4. Very strong tidal currents are known from the Messina Straits between Sicily and Calabria and these are known to affect sediments on the bottom at 1000 m water depth. There is marked bottom erosion across the sill at 100 m depth and giant gravel and sand dunes migrating away from the sill both N and S. These dunes have amplitudes of 10–50 m and although internally structured (laminated and cross-laminated) periodic collapse can lead to more structureless sand units.

Resedimentation from former (Pleistocene) tidal sands along the margin of the straits accumulate in deeper water as both graded and structureless turbidite sands. These "massive" sands are up to 2 m in thickness.

5.3. Massive sand depositional settings

Many of the data summarised in the foregoing discussion on processes, facies, geometry, sequences and modern analogues can be synthesised into four main depositional settings (designated Types I to IV for convenience in this paper only) in which deep-water massive sands occur. Based on a limited number of modern analogues, but coupled with an extensive survey of some 70 ancient examples, for some of which (especially the near-modern ones) the depositional setting is reasonably well known, we are confident in defining these four types (Fig. 16).

5.3.1. Type I: fan delta–braid delta

Massive sands can occur in chutes, channels, flowslides, debris flow tongues and lobe sheets. They are relatively small, proximal systems dominated by

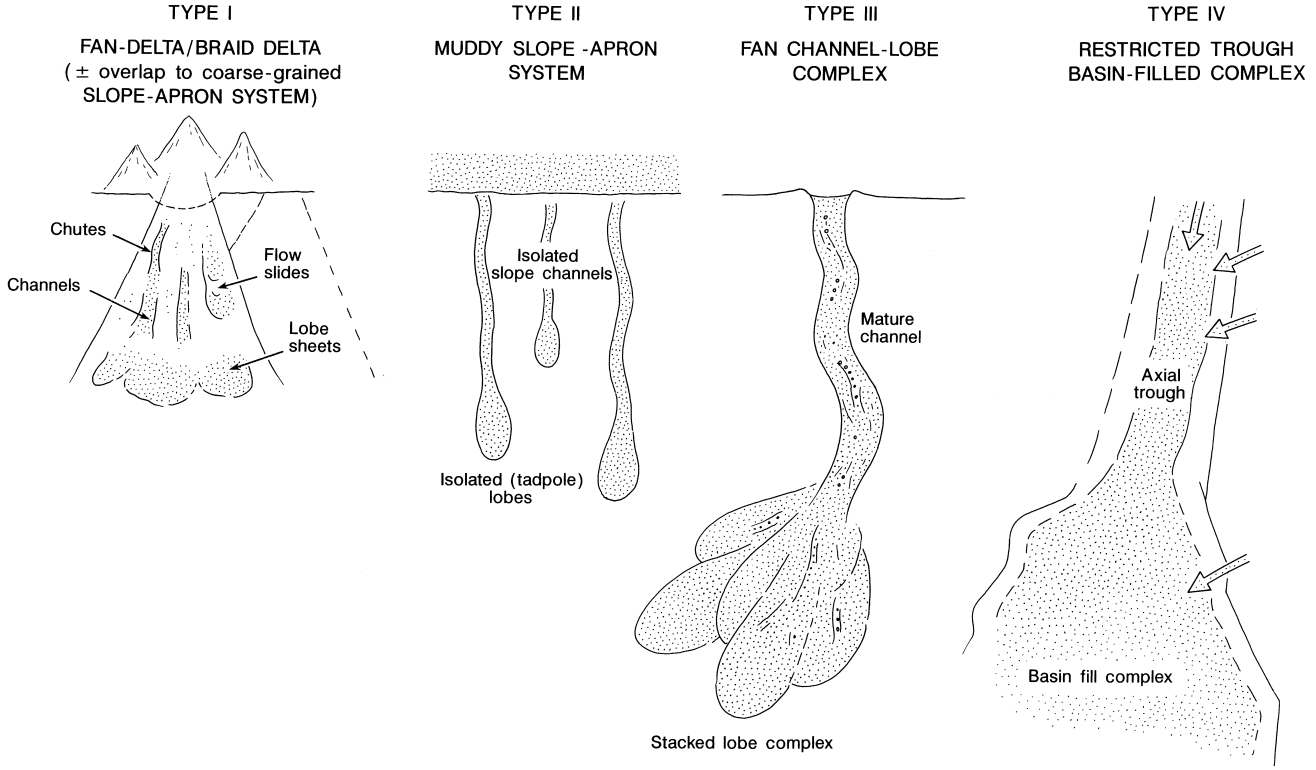

Fig. 16. The four main types of depositional setting identified in this study in which deep-water massive sands occur.

coarse-grained facies of all types. Where several fan/braid delta systems overlap, for example along a tectonically active margin, they form a coarse-grained slope-apron system.

5.3.2. Type II: muddy slope apron

Where a localised shelf-edge sand supply feeds across an otherwise muddy slope apron system, then massive sands can occur in isolated slope channels, debris flow tongues and in the isolated (tadpole) lobes they feed. The sand bodies tend to be very uniform and homogeneous and are typically encased in normal fine-grained slope sediments (hemipelagites and fine turbidites). Post-depositional liquefaction and sand injection is common.

5.3.3. Type III: fan channel–lobe complex

The channel and lobe portions of established submarine fans can contain massive sands and associated turbidite facies where there is an adequate supply of sand and gravel material. Nested channels and lobes occur on younger fans, whereas fully mature channel systems feeding stacked lobe complexes occur on longer established fans. These tend to comprise a wide range of facies types and bed thicknesses together with associated levee, interchannel and lobe fringe turbidites.

5.3.4. Type IV: restricted trough–basin fill complex

The formation of topographically restricted narrow troughs and relatively small basins is typical of many tectonically active areas (e.g. Californian Borderland, young rift systems, arc-related systems, etc). Source area uplift can lead to rapid basin fill by coarse-grained facies and, where a transitional source area flanking the basin has allowed sorting of sand from gravel, thick massive bodies can accumulate. Basin fill may be interrupted by hemipelagic/turbidite shale breaks and/or by megabed input.

The main characteristics of each of these types are more succinctly described in Table 2 and Fig. 16 (plan view). Mesosequences are shown in Fig. 15 and cross-section geometries in Fig. 13. It should be possible to relate any particular massive sand body to one or other of these type models.

6. Summary and hydrocarbon implications

Deep-water massive sands are very thick beds or units (from 1 to over 50 m) of essentially structureless sands or sandstones, that occur in association with turbidites, hemipelagites and other deep-water sediments, and are known to form important subsurface reservoirs for hydrocarbons. Better understanding their nature, variety, geometry and origins has significant implications for the hydrocarbon industry.

Table 2
Deep-water massive sands depositional setting matrix showing principal characteristics associated with each DWMS type

Depositional setting	Massive sand facies assoc.	Facies characteristics					Associated facies	Vertical sequences	Sand body geometry			
		Sst/Sh	Sh. clasts	Texture	Composition	Water Esc			Length/ width	Area (km^2)	Thickness (m)	Shape
Type I — fan/braid-delta (may overlap to form coarse slope apron)	MS (stratified), gravels, immature graded, debrites	> 9:1	±Present	Coarse-grained, poor sorting	Lithic-rich	±Present	Gravels and other c–g facies ± shallow-water facies at top	Irregular	3:1–1:2	< 0.25	< 500	Chute channel, lobe-sheet, flow-slide
Type II — muddy slope apron	MS (water-escape amalgamated units graded–massive)	> 9:1	Common	Medium-grained, mod. sorting	Quartz or QF-rich	Common	Fine hemipelagites ± injection ± turbidites	Blocky, broken–blocky	Ch. 5:1–15:1, lobe 2:1–4:1	< 8	< 100	Isolated channel, isolated (tadpole lobe)
Type III — fan channel–lobe complex	MS (graded), massive-graded, gravels, lower CG beds, slumps, normal turbidites	9:1–5:1	Common	Medium-grained, mod. sorting	Quartz or QFL-rich	Common	Normal turbidites ± hemipelagites ± injection	Fining-up (blockey to stacked), complex, symmetrical	Ch. 5:1–15:1, lobe 2:1–4:1	< 50	< 500	Nested to stacked channels, stacked lobe complex (±tabular)
Type IV — restricted trough–basin complex	MS (all types) amalgamated units, normal turbicilites, megabeds	9:1–7:1	±Present	Medium-grained, med. sorting	Feldspar or QFL-rich	Common	Fine hemipelgites ± turbidites ± megabeds ± shallow-water facies at top	Blocky (±fining-up), (±broken)	Trough 3:1–10:1, basin 3:1–1:2	20–500+	Up to 2000	Trough fill (lensoid to tabular), basin fill (tabular)

6.1. Processes

Massive sands are deposited by a family of related depositional processes that include: (a) *proximal processes* of short duration such as sand creep, flow-slides, grain flow, fluidised flow and liquefied flow, and (b) *long-distance processes* such as sandy debris flows (SDF) and high-density turbidity currents (HDT). Transformation between these and other resedimentation processes is the norm. They do *not* result from deposition or reworking by contour currents or deep tidal currents. From the hydrocarbon perspective, it is important to distinguish between proximal and long-distance transport and between SDF and HDT mechanisms, as the predicted facies associations, internal heterogeneity and architectural attributes will be different. This is not always possible to achieve at present, and further work is needed to refine differences in facies related to processes.

Deposition occurs by one or more of four mechanisms: (a) freezing of an SDF plug, (b) collapse fall-out from the turbulent flow of an HDT, (c) continuous aggradation beneath a sustained HDT, or (d) continuous traction beneath a sustained HDT. These depositional mechanisms may interchange through any one event.

Post-depositional liquefaction and remobilisation is a common secondary process, particularly in moderately thick sand bodies encased in fine-grained lithologies. Reshaping of the sand body margins by sand injection, protrusion and flank steepening occurs. A range of features can be used to show partial but not complete internal remobilisation.

6.2. Facies

Massive sands form part of a Massive Sand Facies Association (MSFA), of which they are an important facies. Their chief characteristics are very thick bedding (2–8 m typical, 20+ m maximum), general absence of internal structures, sharp bed boundaries, rare subtle or partial grading, and a presence of zones with water-escape features, shale clasts, and rare indistinct lamination. They display varied textural and compositional attributes, most typically being poorly to moderately sorted and compositionally relatively immature.

Sequences of water-escape structures can indicate amalgamation of 1–4 m thick beds into much thicker (20–50 m) units. The type and location of shale clasts yields information on depositional process and setting. Post-depositional reworking leaves major traction-current structures. Diagenetic concretions are typically randomly distributed.

Careful analysis of these different attributes can help determine the depositional process, proximality and depositional setting, all of which have important implications for both large-scale geometry of the sand bodies and reservoir-scale heterogeneity.

6.3. Geometry and dimensions

For any one example the MSFA forms a three-dimensional sand body or sand complex. Sand–shale ratios are everywhere in excess of 5:1 and more typically from 7:1 to >9:1. Only some massive sand bodies show good connectivity with other related sand/gravel systems, whereas others are more isolated within mud-dominated systems.

Four main sand body geometries can be identified including: (a) small-scale sand bodies (chutes, shallow channels, lobe sheets, debris flow tongues and flow-slides) with areas <0.25 km^3 and thicknesses <50 m; (b) channel/ribbon sand bodies with areas of 5–35 km^3 and thicknesses of 100–500 m; (c) lobate/lensoid sand bodies ranging up to 50 km^2 in area and 500 m in thickness; and (d) trough-basin sand bodies that are broadly lensoid to tabular in shape and can be up to 500 km^2 in area and over 2000 m thick.

Internal vertical mesosequences tend to be blocky, broken-blocky and blocky-fining upwards in nature (over several tens of metres in thickness). Lobe and basin systems show microsequences characterised by sand compensation cycles, whereas channels show aggradational microsequences.

6.4. Depositional setting

There are four principle depositional settings in which massive sands and MSFAs occur. These are: Type I — fan-delta/braid delta systems, that may overlap to form a sandy slope-apron; Type II — muddy slope aprons with sands in isolated slope channels and tadpole lobes; Type III — fan channel-lobe complexes with mature channels and stacked lobe complexes; and Type IV — restricted trough/basin fill complexes, of relatively small dimensions typical of tectonically active areas. The characteristics and occurrence of these four types are distinctive. A hierarchy of controls determines the development of one or other type, amongst which tectonic activity and ample sand supply figure prominently. Sea level variation does not always have such profound influence. Clearly, the type of depositional setting has profound influence on DWMS reservoir location and characteristics.

Appendix A. References for Fig. 1/Table 1

(*examined by authors this study).

1.* Harding, I. C., et al. (1990). Controls on Eocene

submarine fan deposition in the Witch Ground Graben. *Geol. Soc. (London) Spec. Publ.*, *55*, 353–367.

2. Bernoulli, D., Bichsel, M., Bolli, H. M, Haring, M. O., Hochuli, P. A., & Kleboth, P. (1981). The Missaglia Megabed, a catastrophic deposit in the Upper Cretaceous Bergamo Flysch, northern Italy. *Eclogae Geologicae Helvetiae, 74*, 421–442.

3. Vicente-Brave, J. C., & Robles, S. (1992). Massive sands and gravels in turbidite suites filling a pull-apart basin: Albian from the Basque Cantabrian Basin transtensive rifting, northern Spain. Proceedings of First Arthur Holmes European Research Conference (Geol. Soc. Lond.), Cefalu, Sicily, Abstract Volume, p. 28.

4.* Brindley, J. C., & Schiener, M. E. J. (1973). Sedimentary features of the Bray group, Bray Head, County Wicklow. *The Sci. Proc. Dublin Soc., 27*, 373–389.

5. Nilsen, T. H., & Abbot, P. L. (1981). Paleogeography and sedimentology of Upper Cretaceous turbidites, San Diego, California. *Am. Ass. Pet. Geol. Bull., 65*, 1256–1284.

6.* Case Study 9 — see text references.

7.* Normark, W. R., & Piper, D. J. W. (1971). Reexamination of a Miocene deep-sea fan and fan valley, southern California. *Geol. Soc. Am. Bull., 82*, 1823–1830.

8. Carminatti, M., & Scarton, J. C. (1991). Sequence stratigraphy of the Oligocene turbidite complex of the Campos Basin, Offshore Brazil. In P. Weimer & M. H. Link, (Eds), *Seismic facies and sedimentary processes of submarine fans and turbidite systems* (pp. 241–246). Springer–Verlag.

9.* Case study 10 — see text references.

10. Slacka, A., & Thompson, S. (1981). A revision of the fluxoturbidite concept based on type examples in the Polish Carpathian flysch. *Ann. Soc. Geol. Polon., 51*, 3–44.

11.* Maher, C. E., & Haker, S. D. (1987). Claymore oilfield. In L. V. Illing & G. D. Hobson (Eds.), *Petroleum geology of Northwest Europe* (pp. 835–845). Graham & Trotman.

12.* Hiscott, R. N., & James, N. P. (1985). Carbonate debris flow, Cow Head Group, western Newfoundland. *J. Sedim. Petrol., 55*, 735–745.

13. Nelson, H. E., et al. (1986). A restricted basin with base-of-slope aprons and non-channelised turbidites. *Geology, 14*, 238–241.

14.* Cave, R., Evans, J. A., & Campbell, S. D. G. (1992). Garn Prys: a mid-Silurian canyon feeder to the Denbigh Grits of North Wales. *Geol. J., 27*, 301–315.

15. Walker, R. G. (1977). Deposition of Upper Mesozoic resedimented conglomerates and associated turbidites in SW Oregon. *Bull. Geol. Soc. Am., 88*, 273–285.

16. Crevello, P. D., & Schlager, W. (1980). Carbonate debris sheets and turbidites, Exhuma Sound, Bahamas, *J. Sedim. Petrol., 50*, 1121–1148.

17. Hurst, J. M., & Surlyk, F. (1982). Stratigraphy of the Silurian turbidite sequence of northern Greenland. *Bull. Gronlans, Geol. Under., 145*, 121.

18. Surlyk, F., & Hurst, J. M. (1984). The evolution of the early Paleozoic deep-water basins of northern Greenland. *Bull. Geol. Soc. Am., 95*, 131–154.

19.* Norgard Bolas, H. M. (1987). Odin field. In A. M. Spencer (Ed.), *Geology of the Norwegian oil and gas fields*. Norwegian Petroleum Society.

20.* Waldron, J. W. F., & Jensen, L. R. (1985). Sedimentology of the Goldenville Formation, eastern shore, Nova Scotia. *Geol. Surv. Canada Paper*, 85–15.

21.* Keverlaan, K. (1987). Gordo megabed: a possible seismite in a tortonian submarine fan, Tabernas Basin, Almeria province, SE Spain. *Sedim. Geol., 51*, 165–180.

22. Busby-Spera, C. J. (1988). Evolution of a middle Jurassic back-arc basin, Cedros Island, Baja California: evidence from a marine volcaniclastic apron. *Geol. Soc. Am. Bull., 100*, 218–233.

23.* Case Study 8 — see text references.

24.* Reynolds, J., & Mackay, T. (1992). Post-depositional modification of deep-water sandstones — reservoir geometry of the Gryphon Sand, Gryphon Field, North Sea UK sector 9/18b. Proceedings of First Arthur Holmes European Research Conference (Geol. Soc. Lond.), Cefalu, Sicily, Abstract Volume, p. 19.

25. Cooper, D. J. W. (1990). Sedimentary evolution and paleogeographic reconstruction of the Mesozoic continental rise in Oman. *Geol. Soc. (London) Spec. Pub., 49*, 161–187.

26.* Chough, S. K., Hawan, I. G., & Choe, M. Y. (1990). The Miocene Doumsan fan-delta, SE Korea: a composite fan-delta system in a back arc margin. *J. Sedim. Petrol., 60*, 445–455.

27. Surlyk, F. (1987). Slope and deep shelf gully sandstone, upper Jurassic, east Greenland. *Am. Ass. Pet. Geol. Bull., 71*, 464–475.

28.* Ostwedt, O. J. (1987). Sleipner Ost. In A. M. Spencer (Ed.), *Geology of the Norwegian oil and gas fields*. Norwegian Petroleum Society.

29.* Reeder, M. S., Rothwell, R. G., & Stow, D. A. V. (1999). Influence of sea-level and basin physiography in emplacement of the late Pleistocene Herodotus Basin Megaturbidite, SE Mediterranean. *Marine & Pet. Geol.* (this volume).

30.* O'Driscoll, D. (1992). Tectonic controls on submarine fan morphology: lower Cretaceous Kopervik Sandstone from the Moray Firth Basin, North Sea. Proceedings of First Arthur Holmes European Research Conference (Geol. Soc. Lond.), Cefalu, Sicily, Abstract Volume.

31. Cas, R. A., et al. (1981). The Lower Devonian Kowmung Volcaniclastics: a deep-water succession of

mass flow origin, northeastern Lachlan Foldbelt, NSW. *J. Geol. Soc. Austral., 28*, 271–288.

32. Nemec, W., Porebski, S., & Steel, R. J. (1980). Texture and structure of resedimented conglomerates: excerpts from Ksiaz Formation, SW Poland. *Sedimentol., 27*, 519–538.

33.* Cast Study 6 — see text references.

34. Guardado, L. R., Gamboa, L. A. P., & Lucchesi, C. F. (1990). Petroleum geology of the Campos Basin, Brazil. *Am. Ass. Pet. Geol. Mem., 48*, 3–79.

35.* Ricci Lucchi, F., & Valmori, E. (1980). Basin-wide turbidites in a Miocene, over-supplied deep-sea plain: a geometrical analysis. *Sedimentology, 27*, 241–270.

36.* Case Study 7 — see text references.

37. Cas, R. (1979). Mass flow arenites from a Paleozoic interarc basin, New South Wales, Australia: mode and environment of emplacement. *J. Sedim. Pet., 49*, 29–44.

38.* Stow, D. A. V., et al. (1998). Volcaniclastic sediments: process interaction and depositional setting of the Mio-Pliocene Miura Group, SE Japan. *Sedim. Geol., 115*, 351–382.

39.* Bouma, A. H., Stelting, C., & Coleman, J. C. (1985). Mississippi fan, Gulf of Mexico. In A. H. Bouma, N. E. Barnes, W. R. Normark (Eds.), *Submarine fans and related turbidite sequences* (pp. 143–150). New York: Springer–Verlag.

40.* Stow, D. A. V., et al. (1985). Mississippi fan sedimentary facies, composition, and texture. In A. H. Bouma, N. E. Barnes, W. R. Normark (Eds.), *Submarine fans and related turbidite sequences* (pp. 259–266). New York: Springer–Verlag.

41. Sullwood, H. M. (1960). Tarzana fan: deep submarine fan of late Miocene age, Los Angeles Co., California. *Am. Ass. Pet. Geol. Bull., 44*, 433–457.

42. De Pippo, F., & Valente, A. (1991). Observation forliminan sur conglomerati di Monte Sacro. *Boll. Soc. Geol. It.*, 110.

43.* Kemp, A. E. S., & Kelling, G. (1991). A field traverse of the Southern Uplands Accretionary Terrane, Scotland. Ludlow Research Group Field Excursion Guide, September 1991.

44. Spadini, A. R., et al. (1988). The Macae Formation, Campos Basin, Brazil: its evolution in the context of the initial history of the South Atlantic. *Rev. Bras. Geociencias, 18*, 261–272.

45.* Robertson, A. H. F., et al. (1991). The role of tectonics vs global sea-level change in the Neogene evolution of the Cyprus active margin. *Spec. Publ. Int. Assoc. Sed., 12*, 331–369.

46.* Case Study 5 — see text references.

47.* Case Study 4 — see text references.

48.* Case Study 3 — see text references.

49. AGIP pers. comm. (1992).

50.* Hirayama, J., & Nakajim, T. (1977). Analytical studies of turbidites, Otadai Formation, Boso Peninsula, Japan. *Sedimentology, 24*, 747–764.

51.* Salimullah, A. R. M., & Stow, D. A. V. (1992). Wireline log signatures of resedimented volcaniclastic facies, ODP Leg 129, W Central pacific. *Geol. Soc. (London) Spec. Pub., 65*, 87–97.

52. Busby-Spera, C. (1993). Lithostratigraphy of Cretaceous strata, Cedros Island, Baja California, Mexico. *J. Cret. Res., 14*, 15–21.

53.* Bercowski, F. (1987). Estudio sedimentologico de la Formacion Quebrad de Las Lajas, San Juan Provincia, Argentina. Unpublished PhD thesis, University of Buenos Aires, Argentina.

54.* This study.

55.* Smith, R. D. A. (1988). A sedimentological analysis of the late Llandovery Welsh Basin. Unpublished PhD thesis, University of Cambridge.

56. Johns, D. R., Mutti, E., Rosell, J., & Seguret, M. (1981). Origin of a thick, redeposited carbonate bed in Eocene turbidites, Hecho Group, south central Pyrenees, Spain. *Geology, 9*, 161–164.

57. Cocco, F., et al. (1978). Sedimentologie del Flysch del Cilento — I: le arenarie di Senamezzone. *Geol. Rom., XVII*, 289–302.

58.* Stow, D. A. V., et al. (1984). Depositional model for calcilutites: Scaglia Rossa limestones, Umbro-Marchean Apennines. *Geol. Soc. (London) Spec. Pub., 15*, 223–241.

59.* Kneller, B. C., & McConnell, B. J. (1993). The Seathwaite Fell Formation in the Central Fells. *Brit. Geol. Surv. Tech. Report*, WA93/43.

60.* Kneller, B. C., & McConnell, B. J. (1993). The Seathwaite Fell Formation in the Central Fells. *Brit. Geol. Surv. Tech. Report*, WA93/43.

61. Chippings, D. M. (1972). Sedimentary structures and environment of some thick sandstone beds of turbidite type. *J. Sedim. Pet., 142*, 587–595.

62. Corbet, K. D. (1971). Features of thick bedded sandstone in a proximal flysch sequence, Upper Cambrian, SW Tasmania. *Sedimentology, 19*, 109–114.

63. Cater, J. M. L., Hanna, S. S., Ries, A. C., & Turner, P. (1991). Tertiary evolution of the Sivas basin, central Turkey. *Tectonophysics, 195*, 29–46.

64. Krause, F. F., & Oldershaw, A. E. (1979). Submarine carbonate breccia beds: a depositional model for two-layer sediment gravity flows from the Sekwi Formation (Lower Cambrian), MacKenzie Mountains, NWT, Canada. *Can. J. Earth Sci., 16*, 189–199.

65. Bull, S. W., & Cas, R. A. F. (1991). Depositional controls and characteristics of subaqueous bedded volcaniclastics, Lower Devonian Snowy River volcanics. *Sedim. Geol., 74*, 189–215.

66. Porebski, S. (1992). Personal communication.

67.* Kleverlaan, K. (1989). Three distinctive feeder lobe systems within one time slice on the Tortonian Tabernas fan, SE Spain. *Sedimentology, 36*, 25–45.

68. Wuellner, D. E., & James, W. C. (1989). Braided and meandering submarine channel deposits, Tesnus Formation, Marathon Basin, West Texas. *Sedim. Geol., 62*, 27–45.

69.* Case Study 1 — see text references.

70.* Cast Study 2 — see text references.

References

Allen, J. R. L. (1982). Sedimentary structures: their character and physical basis. *Developments in sedimentology*, *vol. 30A*. Amsterdam: B. Elsevier.

Allen, J. R. L. (1991). The Bouma Division A and the possible duration of turbidity currents. *J. Sedim. Petrol.*, *61*, 291–295.

Ardanese, L. R., Capuano, N., Chiocchini, U., Cipriani, N., Martelli, G., & Veneri, G. T. F. (1987). Studio delle arenarie di Urbania e di Serraspinosa come contributo alla conoscenza dell'evoluzione paleogeografica del margine Adriatico durante il Miocence medio-superiore. Giornale di Geologia, ser 3, Vol 49/1, pp. 127–144, Bologna.

Armstrong, L. A., Ten Have, A., & Johnson, H. D. (1987). The geology of the Gannet field, central North Sea, UK sector. In *Petroleum geology of NW Europe* (pp. 533–548). London: Graham & Trotman.

Barnes, P. M., & Lewis, Y. B. (1991). Sheet slides and rotational failures on a convergent margin: the Kidnappers Slide, New Zealand. *Sedimentology*, *38*, 205–221.

Bouma, A. H., Coleman, J. M., Meyer, A. W. et al (1986). *Init. Repts. DSDP, 96*. Washington (U.S. Govt. Printing Office).

Braakenburg, N. E. (1994). The anatomy of deep water massive sands: with reference to specific examples. Unpublished PhD thesis, University of Southampton, 294 pp.

Bugge, T. (1983). *Submarine slides on the Norwegian continental margin*. Trondheim: Cont. Shelf Inst. publ. 110, IKU 152 pp.

Busby-Spera, C. J. (1985). A sand-rich submarine fan in the lower Mesozoic Mineral King caldera complex, Sierra Nevada, California. *J. Sedim. Petrol.*, *55*, 376–391.

Carman, G. J., & Young, R. (1981). Reservoir geology of the forties oilfield. In *Petroleum geology of the continental shelf of NW Europe* (pp. 371–379). London: Heyden.

Carter, R. M. (1975). A discussion and classification of subaqueous mass transport with particular reference to grain flow, slurry flow and fluxoturbidites. *Earth-Sci. Rev.*, *11*, 145–177.

Chough, S. K., Choe, M. Y., & Hwang, I. G. (1993). Fan deltas in the Pohang Basin, Miocene, SE Korea. In *Field excursion guidebook* (p. 150). Woongjin Publisher.

Elliott, T., Apps, G., Davies, H., Evans, M., Ghibaudo, G., & Graham, R. H. (1985). A structural and sedimentological traverse through the Tertiary Foreland basin of the external Alps of France. In *Excursion guidebook, International Symposium on Foreland Basins*. Switzerland: Fribourg.

Enjolras, J. M., Gouadain, J., Mutti, E., & Pizon, J. (1986). New turbidite model for the Lower Tertiary sands in the southern Viking Graben. In *Habitat of hydrocarbons on the Norwegian continental shelf, Norwegian Petroleum Society* (pp. 171–178). London: Graham & Trotman.

Flood, R., Piper, D. J. W. et al. (1995). ODP Initial Reports 155, Texas, Ocean Drilling Program.

Flood, R., Piper, D. J. W. et al. (1997). ODP Scientific Results 155, Texas, Ocean Drilling Program.

Gee, M. R. J., Masson, D. G., Watts, A. B., & Allen, P. A. (1999). The Saharan Debris Flow: an insight into the mechanics of long runout debris flows. *Sedimentology, 46*, 317–336.

Graham, S. A., & Berry, K. D. (1979). Early Eocene paleogeography of the central San Joaquin Valley — origin of the Cantua Sandstone. *Cenozoic paleogeography of the Western United States, SEPM Pacific Section, Paleogeography Symposium*, *vol. 3* (pp. 119–128).

Hampton, M. A. (1972). The role of subaqueous debris flow in generating turbidity current. *J. Sedim. Petrol.*, *42*, 775–793.

Hein, J. F. (1982). Depositional mechanisms of deep-sea coarse clastic sediments, cap Enrage Formation, Quebec. *Can. J. Earth Sci.*, *19*, 267–287.

Heller, P. L., & Dickinson, W. R. (1985). Submarine ramp facies model for delta fed, sand-rich turbidite systems. *Am. Ass. Petrol. Geol. Bull.*, *69*, 960–976.

Hoyez, B. (1989). Le Numidien et les flysch oligomiocene de la bordure sud de la Mediterranee occidentale. Unpublished PhD thesis, University of Lille, France.

Hughes Clarke, J. E., Shor, A. N., Piper, D. J. W., & Mayer, L. A. (1990). Large-scale current-induced erosion and deposition in the path of the 1929 Grand Banks turbidity current. *Sedimentology*, *37*, 613–629.

Ito, M. (1992). High frequency depositional sequences of the upper part of the Kasuza Group: a middle Pleistocene forearc basin fill in Boso Peninsula, Japan. *Sedim. Geol.*, *76*, 155–175.

Ito, M., & Katsura, Y. (1992). Inferred glacioeustatic control for high frequency depositional sequences of the Plio-Pleistocene Kasuza Group, a forearc basin fill in Boso Peninsula, Japan. *Sedim. Geol.*, *80*, 67–75.

Johansson, M., & Stow, D. A. V. (1995). A classification scheme for shale clasts in deep-water sandstones. *Geol. Soc. (London) Spec. Pub.*, *94*, 221–241.

Johansson, M., Braakenburg, N. E., Stow, D. A. V., & Faugeres, J. C. (1998). Deep-water massive sands: facies, processes and channel geometry in the Numidian Flysch, N Sicily. *Sedim. Geol.*, *115*, 233–266.

Kneller, B. (1995). Beyond the turbidite paradigm: physical models for the deposition of turbidites and implications for reservoir prediction. *Geol. Soc. (London) Spec. Pub.*, *94*, 221–241.

Kneller, B., & Branney, M. J. (1995). Sustained high-density turbidity currents and the deposition of thick massive beds. *Sedimentology*, *42*, 607–616.

Lee, J. H. (1989). Undersea landslides: extent and significance in the Pacific Ocean. In *Proceedings of 28th International Geological Congress, Symposium on Landslides* (pp. 367–380).

Link, M. H. (1975). Matilija Sandstone, a transition from deep-water turbidite to shallow-marine deposition in the Eocene of California. *J. Sedim. Petrol.*, *45*, 63–78.

Link, M. H., & Nilsen, T. H. (1980). The Rocks Sandstone, an Eocene sand-rich deep-sea fan deposit, northern Santa Lucia Range, California. *J. Sedim. Petrol.*, *50*, 583–601.

Link, M. H., & Welton, J. E. (1982). Sedimentology and reservoir potential of Matilija Sandstone: an Eocene sand-rich deep sea fan and shallow marine complex, California. *Am. Ass. Petro. Geol. Bull.*, *66*, 1514–1534.

Link, M. H., Squires, R. L., & Colburn, I. P. (Eds.). (1981). *Simi Hills Cretaceous turbidities, southern California. SEPM Pacific Section, Fall Fieldtrip Guidebook* .

Lowe, D. R. (1976). Subaqueous liquefied and fluidised sediment flows and their deposits. *Sedimentology*, *23*, 285–308.

Lowe, D. R., & Lopiccolo, R. D. (1974). The characteristics and origins of dish and pillar structures. *J. Sedim. Petrol.*, *44*, 484–501.

Masson, D. G., Kenyon, N. K., & Weaver, P. P. E. (1996). Slides, debris flows and turbidity currents. In *Oceanography — an illustrated guide* (pp. 136–151). London: Manson Publishing.

Masson, D. G., van Niel, B., & Weaver, P. P. E. (1997). Flow processes and sediment deformation in the Canary debris flow on the NW African continental rise. *Sedim. Geol.*, *110*, 163–179.

Middleton, G. V., & Hampton, M. A. (1976). Subaqueous sediment transport and deposition by sediment gravity flows. In *Marine*

sediment transport and environmental management (pp. 197–218). New York: John Wiley.

Mohrig, D., Whipple, K. X., Hondzo, M., Ellis, C., & Parker, G. (1998). Hydroplaning of subaqueous debris flows. *Geol. Soc. Am. Bull.*, *110*, 387–394.

Mutti, E., Barros, K., Possato, S., & Rumenos, L. (1980). Deep-sea fan turbidite sediments winnowed by bottom currents in the Eocene Campos Basin, Brazil offshore. In *Proceedings of first IAS European Meeting Abstracts* (p. 114).

Mutti, E., Davoli, G., SegadeUi, S., Cavaffi, C., Carminatti, K., Stocchi, S., Mora, S., & Andreozzi, M. (1992). *Turbidite sandstones*. Parma: AGIP/Istituto di Geologia, Universita di Parma 236 pp.

Nelson, C. H., Baraza, J., & Maldonado, A. (1993). Mediterranean undercurrent sandy contourites, Gulf of Cadiz, Spain. *Sedim. Geol.*, *82*, 103–131.

Nemec, W. (1990). Aspects of sediment movement on steep delta slopes. *Spec. Publ. Int. Ass. Sediment.*, *10*, 29–73.

Nilsen, T. H., Dibblee, T. W., & Simoni, T. R. (1974). In *Stratigraphy and sedimentation of the Cantua Sandstone of the Lodo Formation, Valecitos area, California. SEPM Pacific Section guidebook* (pp. 38–68).

Parise, O., & Beaudoin, B. (1986). Les filons greseux du Numidien dans leur cadre paleomorphologique (Sicile et Tunise). *C.R. Acad. Sci. Paris*, *304*, 129–134.

Parise, O., Beaudoin, B., & Fries, G. (1999). Deep-water massive sands: facies, processes and channel geometry in the Numidian Flysch, Sicily — a discussion. *Sedim. Geol.* (this volume).

Pettingill, H. S. (1998). Turbidite giants: lessons from the world's 40 largest turbidite discoveries. In *Proceedings of EAGE/AAPG Third Research Symposium, Almeria, Spain* Abstracts Volume AO27.

Pickering, K. T., Hiscott, R. N., & Hein, F. J. (1989). *Deep marine environments: Clastic sedimentation and tectonics*. London: Unwin Hyman 416 pp.

Piper, D. J. W. (1970). Transport and deposition of Holocene sediment on La Jolla deep sea fan, California. *Marine Geol.*, *8*, 211–227.

Piper, D. J. W., & Savoye, B. (1993). Processes of turbidity current flow and deposition on the Var deep-sea fan, NW Mediterranean Sea. *Sedimentology*, *40*, 557–582.

Piper, D. J. W., Normark, W. R., & Stow, D. A. V. (1984). The Laurentian fan — Sohm abyssal plain. *Geo-Marine Letters*, *3*, 141–146.

Pirmez, C., Hiscott, R. N., & Kronen, D. (1997). Sandy turbidite successions. *Proc. ODP Sci. Results*, *155*, 7–34.

Postma, G. (1984). Mass-flow conglomerates in a submarine canyon: Abrioja fan-delta, Pliocene, SE Spain. *Mem. Can. Soc. Petrol. Geol.*, *10*, 237–258.

Postma, G., Nemec, W., & Kleinspehn, K. L. (1988). Large floating clasts in turbidites: a mechanism for their emplacement. *Sedim. Geol.*, *58*, 47–61.

Roure, F., Howell, D. G., Muller, C., & Moretti, I. (1990). Late Cenozoic subduction complex of Sicily. *J. Struct. Geol.*, *12*, 259–266.

Simpson, J. E. (1982). Gravity currents in the laboratory, atmosphere and ocean. *Ann. Rev. Fluid Mech.*, *14*, 213–234.

Southard, J. E., & Mackintosh, M. E. (1981). Experimental test of autosuspension. *Earth Surface Proc. Landf.*, *6*, 103–111.

Shanmugam, G. (1996). High-density turbidity currents: are they sandy debris flows? *J. Sedim. Research*, *66*, 2–10.

Shanmugam, G. (2000) Fifty years of the turbidite paradigm: Deep-water processes and facies models – a critical perspective. *Marine & Petrol. Geol.*, this issue.

Shanmugam, G., & Moiola, R. J. (1995). Re-interpretation of depositional processes in a classic flysch sequence (Pennsylvanian Jackfort Group), Ouachita Mountains, Arkansas and Oklahoma. *Am. Ass. Pet. Geo. Bull.*, *79*, 672–695.

Shanmugam, G., & Moiola, R. J. (1997). Re-interpretation of depositional processes in a classic flysch sequence (Pennsylvanian Jackfort Group), Ouachita Mountains, Arkansas and Oklahoma: reply. *Am. Ass. Pet. Geol. Bull.*, *81*, 476–491.

Shanmugam, G., Lehtonen, L. R., Straume, T., Syversten, S. E., Hodgkinson, R. J., & Skibeli, M. (1994). Slump and debris flow dominated upper slope facies in the Cretaceous of the Norwegian and Northern North Seas: implications for sand distribution. *Am. Ass. Pet. Geol. Bull.*, *78*, 910–937.

Stanley, D. J., Palmer, H. R., & Dill, R. F. (1978). Coarse sediment transport by mass flow and turbidity current processes and downslope transformations in Annot Sandstone canyon-fan valley system. In *Sedimentation in submarine canyons, fans and trenches* (pp. 85–115). Pennsylvania: Dowden, Hutchinson & Ross.

Stow, D. A. V. (1981). The Laurentian Fan: morphology, sediments, processes and growth pattern — models for hydrocarbon exploration. *Am. Ass. Pet. Geol. Bull.*, *65*, 375–393.

Stow, D. A. V. (1994). Deep sea processes of sediment transport and deposition. In *Sediment transport and depositional processes* (pp. 257–291). Oxford: Blackwell Sci. Pub.

Stow, D. A. V., Braakenburg, N. E., & Johansson, M. (1995). Atlas of deep-water massive sands. Unpub. Rept., Southampton University.

Stow, D. A. V., Reading, H. G., & Collinson, J. (1996). Deep seas. In *Sedimentary environments and facies* (pp. 380–442). Blackwell Sci. Publ.

Stow, D. A. V., Cremer, M., Droz, L., Normark, W. R., O'Connell, S., Pickering, K. T., Stelting, C. C., Meyer-Wright, A. A., & DSDP Leg 96 Shipboard Scientists (1985). Mississippi Fan Sedimentary facies, composition, and texture. In *Submarine fans and related turbidite sequences* (pp. 259–266). New York: Springer–Verlag.

Stow, D. A. V., Faugeres, J. C., Viana, A., & Gonthier, E. (1998). Fossil contourites: a critical review. *Sedim. Geol.*, *155*, 3–31.

Stow, D. A. V., Johansson, M., Braakenburg, N. E., & Faugeres, J. C. (1999). Deep-water massive sands: facies, processes and channel geometry in the Numidian Flysch, N Sicily: Reply. *Sedim. Geol., 127*, 119–123.

Surlyk, F. (1987). Slope and deep shelf gully sandstones, Upper Jurassic, East Greenland. *Am. Ass. Pet. Geol. Bull.*, *71*, 464–475.

Viana, A., Faugeres, J. C., & Stow, D. A. V. (1998). Bottom-current controlled sand deposits: a review of modem shallow to deep water environments. *Sedim. Geol.*, *115*, 53–80.